RESEARCH ON AN INVESTIGATION INTO SULPHUR CHEMISTRY WITH SPECIFIC APPLICATION TO BIOLOGICAL SULPHATE REMOVAL PROCESSES

Report to the
Water Research Commission

by

RE Loewenthal, B Morgan, O Lahav and G Hearne

on behalf of the
University of Cape Town

WRC Report No. 1079/1/08
ISBN 978-1-77005-040-2

OCTOBER 2008

DISCLAIMER

This report has been reviewed by the Water Research Commission (WRC) and approved for publication. Approval does not signify that the contents necessarily reflect the views and policies of the WRC, nor does mention of trade names or commercial products constitute endorsement or recommendation for use.

EXECUTIVE SUMMARY

The principal aims to this contract were threefold:

i. to investigate and model a sulphide chemistry in both the aqueous and gaseous phases,
ii. to investigate and model the recovery of elemental sulphur through chemical oxidation of sulphide, and
iii. to investigate and model the precipitation and recovery of metals.

With regard to sulphide chemistry, this is complex and governed by both weak acid and redox reactions.

In Acid Mine Drainage (AMD) waters, this is further complicated by the co-existence of both the carbonate, hydroxide and base systems. The only reasonable approach to understanding is via equilibrium chemistry. This is effected here in a clear and didactic fashion, using graphical approaches effected in so-called equilibrium diagrams. This approach is extended to examining interphase equilibrium, for example aqueous-solid phase chemistry of the redox and weak acid reactions of both metal sulphides and elemental sulphur.

Consideration is given to the feasibility of developing a unit process to effect elemental sulphur recovery using physico-chemical methods. Aspects investigated included measurement of hydrogen sulphide (H_2S) stripping using CO_2 or the stripping agent. The H_2S was then oxidized to elemental sulphur by passing the carrier gas through a ferric solution. The rapid kinetics of the various processes make this proposal worthy of further investigation.

With regard to precipitation and recovery of metals, two important findings were identified. First, the flocculation effect observed in the Rhodes BioSURE System was found to be caused by a ferric / ferrous / sulphate / hydroxide – better known as Green Rust which is a metastable precipitant. This floc decomposes within a day to magnetite, haematite and other ferrous / ferric minerals. Further investigation into the decomposition process led us to a unique method of producing magnetite (ferrite) from AMD waters, a process effected at ambient temperature using air as oxidant. This aspect has been further investigated under a separate WRC contract and the process patented by the WRC.

ACKNOWLEDGEMENTS

The authors wish to thank the Water Research Commission of South Africa who provided financial assistance for this research. Special thanks are also given to all the members of the WRC Steering Committee who gave their time and many helpful suggestions during the course of this research. They are Mr GN Steenveld (Chairman), Dr DR Arnold, Dr C Brouckaert, Professor CA Buckley, Professor G Ekama, Professor GS Hansford, Dr A E Lewis, Dr A Neba, Professor PD Rose, Dr JP Smit and Mr O Hempel (Committee Secretary). The authors also wish to thank Ms R Wolson of the Research and Innovation Office of the University of Cape Town for her contribution towards acquiring patent rights for this research. Finally, Mr N Lakay is thanked for assisting in the laboratory.

TABLE OF CONTENTS

CHAPTER 1

INTRODUCTION

Acid mine drainage (AMD) waters are characterized by low pH, very high dissolved iron concentration, dangerously high concentrations of non-ferrous metals (mainly heavy metals), and very high salinity principally in the form of sulphate. This chemical composition of AMD results from a biogeochemical process in which mining operations allow atmospheric oxygen and water to come into contact with rock/material so that aerobic bacteria cause oxidation of iron pyrite (Fe S_2) present in the rock. This oxidation process releases sulphate, protons and ferrous species into underground waters. The resultant low pH causes further leaching of non-ferrous metals from the rock. The type and concentrations of these other metals varies with the local geology.

AMD waters impact negatively on fresh water resources in mining areas of South Africa and many other parts of the world. A comprehensive solution to this pollution requires pH neutralization and removal of both metal and sulphate species. Current practice in South Africa involves using either purely physico-chemical processes or biochemical processes.

Physico-chemical processes include the High Density Sludge Process (HDS) and the Ambient Temperature Ferrite (ATF) Process (developed in part from the work reported here) for metal ion removal; lime and limestone acid neutralization process and the Slurry Precipitation and Recycle Reverse Osmosis (SPARRO) process. However, all these treatment processes (except for the ATF process) generate large volumes of unstable metal hydroxide/oxide sludges which are costly to dispose of and require hazardous waste sites. Further, within these processes mineral precipitation may result in fouling problems of pipes and membranes. These factors together tend to make the processes very expensive and difficult to operate.

With regard to biochemical treatment methods, a number of these have been proposed for use in South Africa – invariably these involve one or more of the following processes:

i. Biological reduction of sulphate to sulphide using some organic compound(s) as electron donor.
ii. Precipitation of metal ions with both the biologically generated sulphide species and hydroxide/oxides – thereby removing both undesirable cationic and anionic species.
iii. Partial oxidation of the biologically generated sulphide species to elemental sulphur – an economical desirable by-product of the process.

In South Africa the importance of the above processes is highlighted by the proposed Rhodes BioSURE System, a physio-biochemical means for the treatment of AMD waters. The various processes underpinning the Rhodes BioSURE System may be summarized briefly as follows:

i. Primary settled sewerage sludge is used as an electron donor for biological sulphate reduction of a fraction of the AMD flow;
ii. the sulphides generated are blended with the remaining AMD flow with resultant precipitation of ferrous and heavy metals;
iii. the blending precipitation reactions above, together with line addition, cause a concomitant flocculation affect (shown in this work to be green rust) which enmeshes suspended precipitants and other suspended solids in an efficient clarification process;

iv. remaining sulphides are partially oxidized to elemental sulphur. Furthermore, the overall reduction reactions within this system results in proton utilization (alkalinity generation) enhancing pH neutralization.

Irrespective of whether a physio-chemical or biochemical approach is adopted to AMD water treatment, an understanding of the chemistry underpinning the systems is necessary so that process design and optimization can be effected. The chemistry of AMD waters is governed largely by pH-redox equilibrium chemistry of the sulphur system, the metal ion systems present, as well as the influence of the carbonate system in the aqueous, solid and gas phases. This chemistry is complex and very difficult to understand and interpret in terms of AMD water environment. Consequently, a large fraction of this research report is dedicated to presentation of the pertinent equilibrium chemistry. Graphical approaches are adopted and these form a simple means of presentation in an easily understood didactic fashion (Chapter 2 and Chapter 5).

In Chapter 3 aspects of the practical problem of physico-chemical removal of sulphate from water are considered. In particular, accepting that sulphate is reduced first to sulphide as effected in the Rhodes BioSURE System. Two approaches to removal of sulphides are considered. First, passive diffusion of gaseous sulphide across a permeable silicone membrane. Second, stripping of sulphide species using CO_2 as a sperger and carrier gas. Thereafter, recovery practicalities of elemental sulphur from the sulphide are considered.

In Chapter 4 and 5 the occurrence of coagulation and flocculation, within the Rhodes BioSURE System, is discussed. This investigation required consideration of some aspects of hydroxide/oxide and sulphide mineral precipitation chemistry using equilibrium and quasi-equilibrium chemistry. The occurrence of green rust (a ferric/ferrous sulphato-hydroxide) is considered, together with the nature of this quasi-equilibrium mineral, as a precursor to magnetite/ferrite.

CHAPTER 2
THE SULPHIDE, IRON AND CARBONATE SYSTEMS - EQUILIBRIUM CHEMISTRY – A GRAPHICAL APPROACH

Before explicitly dealing with metal sulphate-sulphide and sulphur aqueous systems it is necessary to review briefly the chemistry of such systems. In this respect equilibrium chemistry forms the ideal framework for enquiry – in particular, utilization of graphical description forms an extremely useful didactic mechanism. Once completed, the more general engineering implications are addressed in following chapters.

2.1 THE SULPHIDE/SULPHATE/SULPHUR SYSTEM

2.1.1 Aqueous phase equilibrium

The aqueous phase equilibrium chemistry of the sulfur system is governed by equilibria relationships for both weak acid and redox relationships. In addition mass balance and various capacity equations can be formulated. A summary for these equilibrium weak acid relationships is

$$K_1 = \frac{[HS^-][H^+]}{[H_sS]} \tag{2.1}$$

$$K_2 = \frac{[S^{2-}][H^+]}{[HS^-]} \tag{2.2}$$

The equilibrium redox relationships are

$$K_3 = \frac{[SO_4^{2-}][H^+]^{10}[e]^8}{[H_2S]} \tag{2.3}$$

$$\frac{K_4 = [SO_4^{2-}][H^+]^9[e]^8}{[HS^-]} \tag{2.4}$$

The mass balance expressions is

$$S_T = [H_2S] + [HS^-] + [SO_4^{2-}] \tag{2.5}$$

The various redox capacity relationships can be formulated from electron balance considerations with arbitrarily selected reference species. Such equations are important in establishing solutions to modeling kinetics. At low redox potential (SO_4^{2-} negligible), the

distribution of species with pH is plotted using Equations 2.1 and 2.2 as depicted in Figure 2.1.

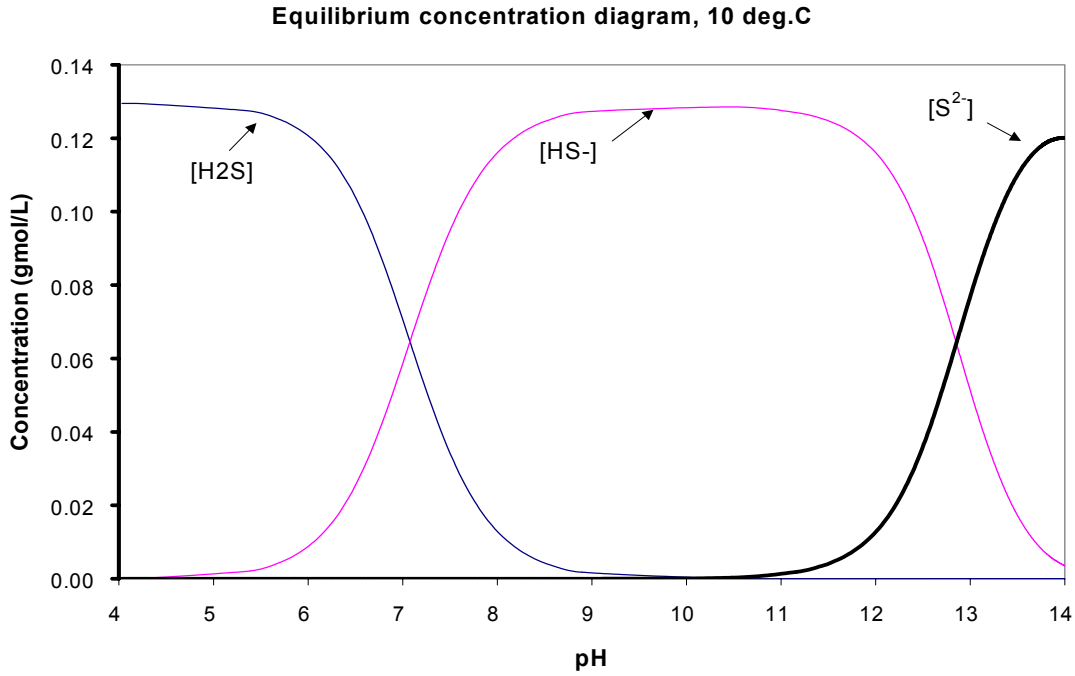

Figure 2.1 Distribution of sulphide species with pH at 10°C.

The distribution of species with redox potential at low pH (i.e. HS^- negligible) can be plotted using Equations 2.3 and 2.5 as depicted in Figure 2.2.

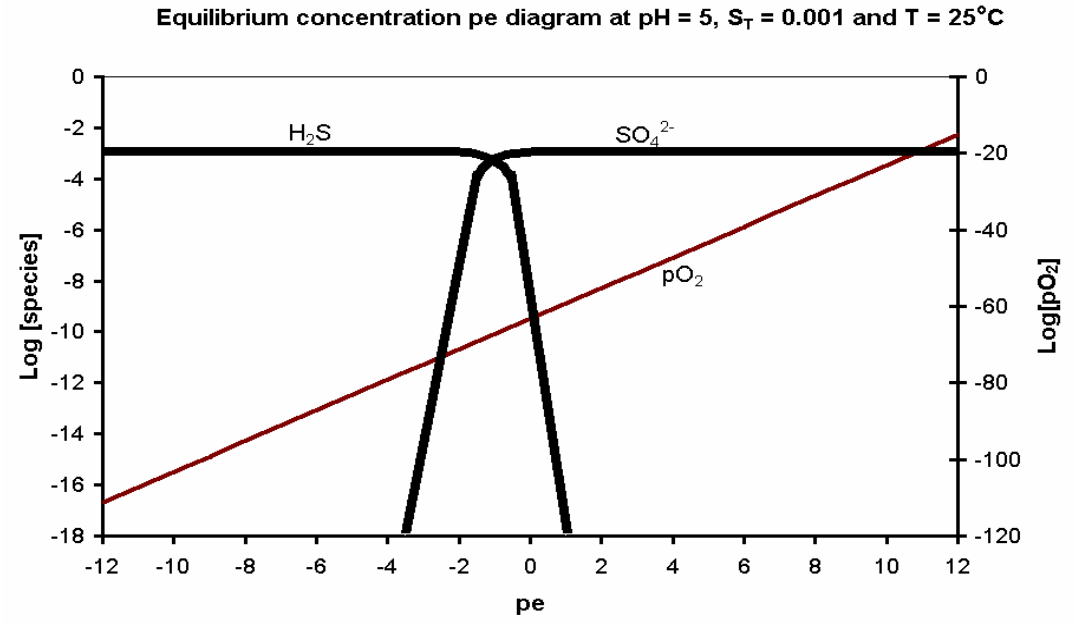

Figure 2.2 Effect of pe on the concentrations of H_2S and SO_4^{2-} at pH = 5.

A similar plot can be affected at a high pH (where H_2S is negligible). Also plotted in Figure 2.2 is a line representing dissolved O_2 with redox potential for H_2O equilibrium at pH = 5.

Referring to Figure 2.2, clearly for H_2S_{aq} in equilibrium with the air (pO_2 = 0.21 atmospheres), the totally dominant sulphur species is SO_4^{2-}.

2.1.2 Aqueous-gas phase equilibrium

For aqueous-gas equilibrium, one can introduce a further equilibrium expression i.e. Henry's law equation to those listed above for interphase equilibrium.

$$H_2S = K_H\, pH_2S \qquad (2.6)$$

At low redox potential the distribution of species with pH is shown plotted in Figure 3 for pH_2S equal to 0.21 atmospheres.

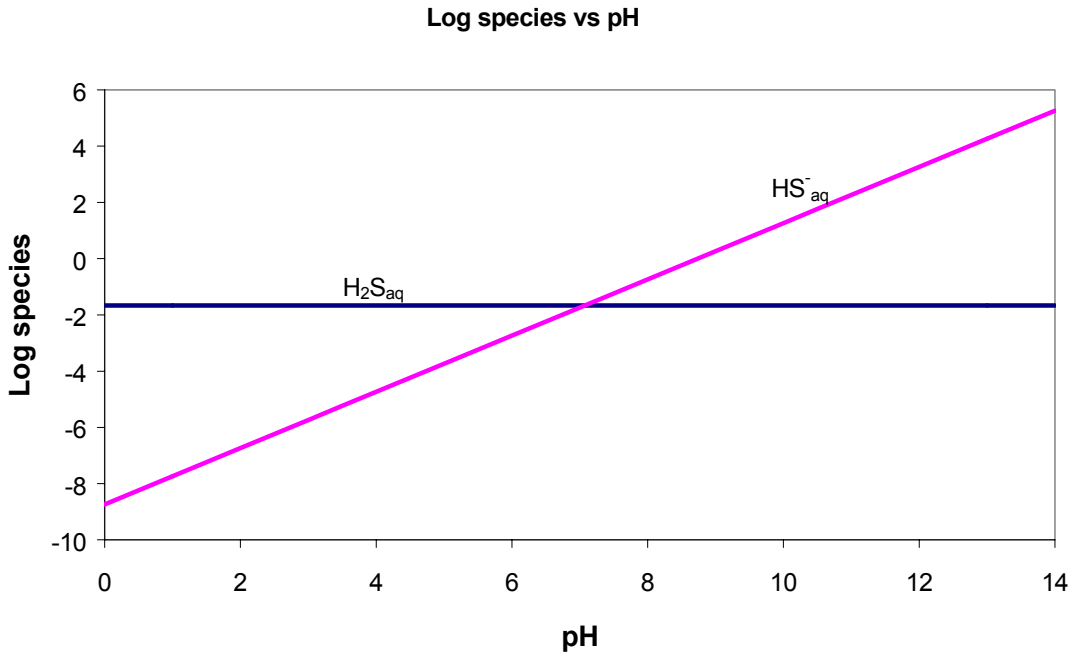

Figure 2.3 Solubility of reduced sulfur species at pH_2S = 0.21 atmospheres

Similarly, at high redox potentials, a log species – pe diagram can be constructed for a fixed pH. However, such a plot has no use within the context of the work reported here and is omitted.

2.1.3 Aqueous-solid phase equilibrium

The solid phase of interest to this investigation is elemental sulphur, and the relevant equilibrium equation, at low pH, is between H_2S and S^o

$$K_s = \frac{[H^+]^2[e]^2}{[H_2S]} \tag{2.7}$$

At higher pH, an equation relating HS^- and S^o species is

$$Ks = \frac{[H^+][e]^2}{[HS^-]} \tag{2.8}$$

The maximum concentration of dissolved sulphur species at low redox levels (say pe -3, i.e. SO_4^{2-} is negligible, see Figure 2.2) is shown plotted in Figure 2.4.

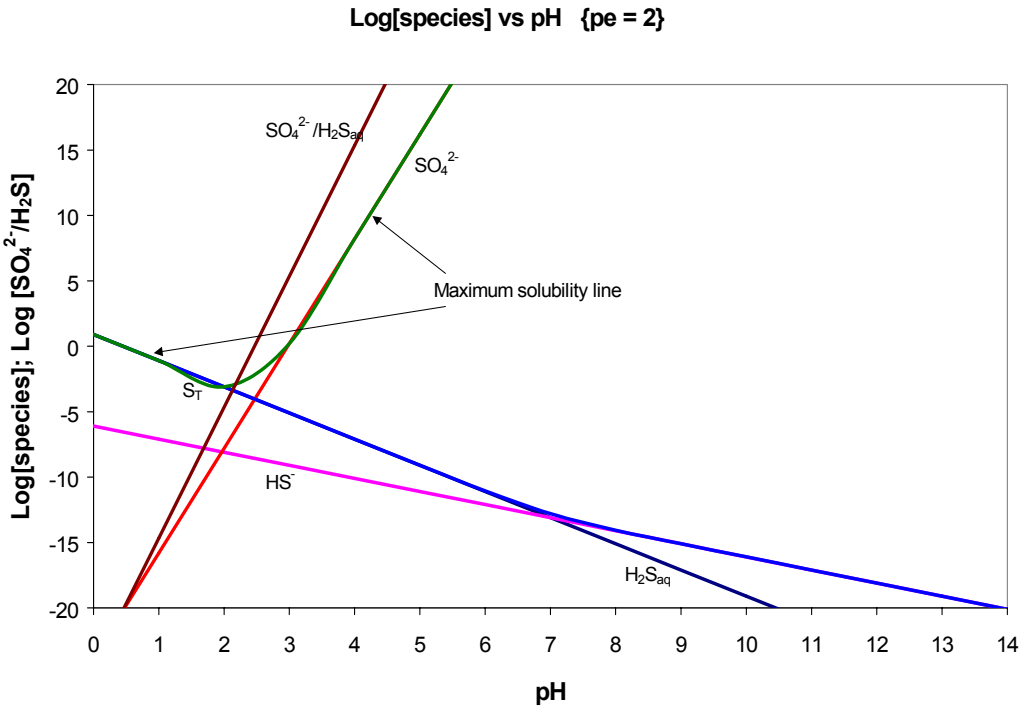

Figure 2.4 Solubility of reduced sulphur species at very low redox levels, pe = -3

The affects of redox potential on the solubility of species require considering the relationship between SO_4^{2-} and S^o, i.e.

$$K = 1 / ([SO_4^{2-}][H^+][e]^6) \tag{2.9}$$

This relationship could be superimposed on figure 2.4 to give a plot for total dissolved sulphur species with species at a fixed selected Pe value. (this is shown in figure 2.5 for Pe = 5).

Recognising that the objective of this work is removal of sulphur species from solution via sulphur formation, from an equilibrium standpoint this is possible, see Figure 2.5. The relative concentrations of oxidised and reduced species can be obtained from the aqueous phase considerations between H_2S and SO_4^{2-} i.e. Equation 2.3 to give the ratio of SO_4^{2-} to H_2S with pH at a fixed redox value. This line is shown superimposed on Figure 2.5.

The presentation above for aqueous –solid phase equilibrium gives a description of the sulphur system with pH at a fixed pe. Alternatively a similar type of diagram can be effected for variable pe and fixed pH. This is shown in Figure 2.6 in a log species – pe plot with pH = 2.

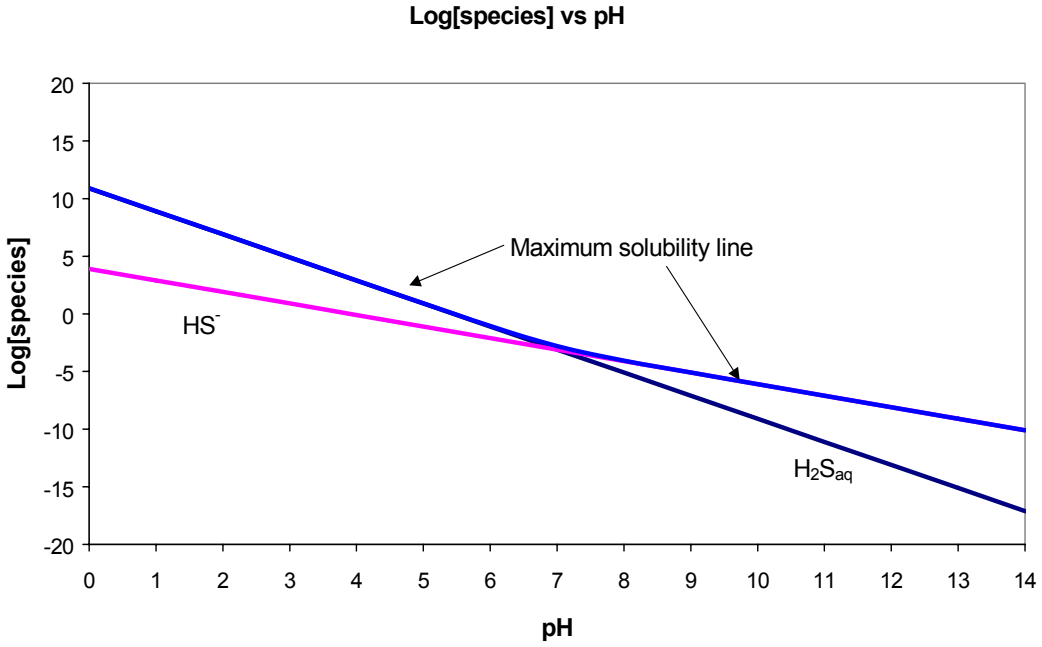

Figure 2.5 Reduced sulphur species, S^o and SO_4^{2-} at pe = 2. The plot gives total dissolved species concentration

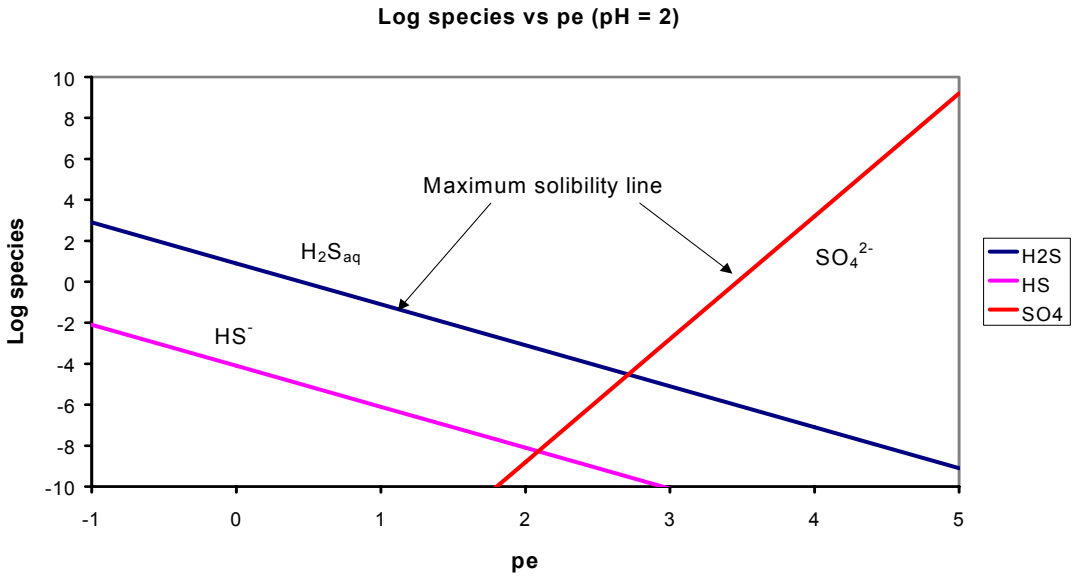

Figure 2.6 Solubility of dissolved sulphur species with redox potential at pH = 2

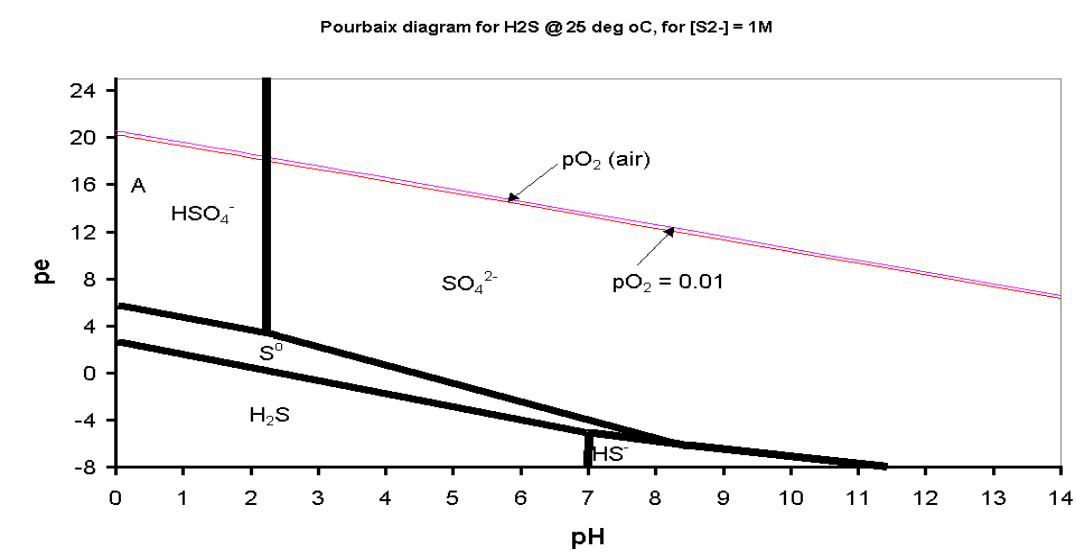

Figure 2.7 Pourbaix diagram with maximum dissolved S species equal to 1 M

Although Figures 2.5 and 2.6 are extremely useful in depicting maximum solubility of sulphur species in solution at aqueous – solid phase equilibrium, a more general presentation of the system is one which has variable pe and pH, and depicts domains of dominance of the various sulphur species. This diagram is called the Pourbaix diagram. In Figure 2.7, is a plot for the $H_2S/HS^-/SO_4^{2-}$ /S system with maximum concentration of dissolved sulphur species equal to 1 M.

The merit of such a diagram is that it presents the overall structure of the system thereby giving an overview to the system, however, it does not quantify either the expected solubility

of sulphur species or the concentration of various sulphur species in solution. These are readily obtained from the plots given in Figures 2.5 and 2.6.

The work above presents a system in which reduced S species are partially oxidised either to elemental sulphur or more completely to HSO_4^{2-} and SO_4^{2-} i.e. a presentation of the oxidation step in some overall redox reaction. However the reduction step should also be considered. In practice the oxidant is invariably either O_2 or ferric and the role of these species are now considered.

2.1.4 Chemistry of the iron system in relation to the oxidation of the reduced S species

The equation for the half reaction in reduction of ferric is

$$K = \frac{[Fe^{2+}]}{[Fe^{3+}][e^{-}]} \tag{2.10}$$

For oxygen

$$K = \frac{1}{pO_2[H^{+}]^4[e]^4} \tag{2.11}$$

These relations can be depicted in a Pourbaix diagram as shown in Figure 2.8. Also shown in Figure 2.8 are the insoluble ferric and ferrous hydroxides, $Fe(OH)_2$ and $Fe(OH)_3$ (fresh precipitates). Lines representing dissolved O_2 in equilibrium with both the air (pO_2 = 0.21 atm.) and a gas with pO_2 = 0.01 atmosphere are also shown in this plot.

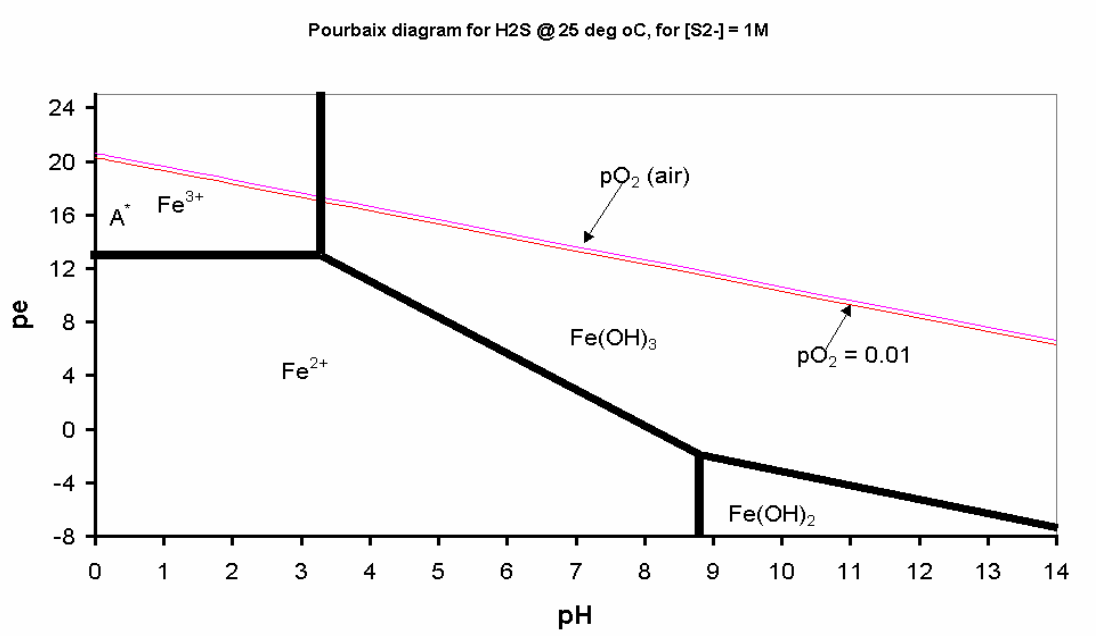

Figure 2.8 Pourbaix diagram with maximum dissolved Fe^{3+} species equal to 10^{-4} M

It is now possible to inquire into the oxidation of reduced sulphur species with excess ferric as oxidant, and alternatively with oxygen as an oxidant. This is achieved by superimposing the Pourbaix diagram for the sulphur system onto the ferric system. With regard to the Fe^{3+} compartment, the redox level will be greater than about pe =13.1. However, transferring a pe value of 13.1 onto the sulphur diagram indicates a domain in which SO_4^{2-}/ HSO_4^{2-} is totally dominant, points A and A^* in Figure 2.7 and 2.8 respectively. Where O_2 is the electron acceptor, the redox is even higher and further into the SO_4^{2-}/ HSO_4^{2-} domain on the sulphur diagram. However, referring to work reported in the literature, elemental sulphur forms in such a system operating at pH = 2. Consequently, one must conclude that equilibrium thermodynamics is not the governing criterion and that kinetics of oxidation of H_2S to S^o is very much faster than S^o to SO_4^{2-}. This hypothesis has also been postulated by Janssen for biological systems (Janssen et al., 1998). Furthermore, the kinetics of oxidation of H_2S directly to SO_4^{2-} at the operating pe value is also slow compared with that to S^o. This is an important conclusion and would indicate that further research should be directed towards modeling of the kinetics of processes involving elemental S recovery.

2.2 THE CARBONATE SYSTEM AND THE ROLE OF CO_2 IN THE H_2S STRIPPING PROCESS

The equilibrium equations for the carbonate subsystem are given in Equations 2.12 to 2.14

$$(H^+)\cdot[HCO_3^-] / [H_2CO_3^*] = K'_{C1} \quad (2.12)$$

$$(H^+)\cdot[CO_3^{2-}] / [HCO_3^-] = K'_{C2} \quad (2.13)$$

$$C_T = [H_2CO_3^*] + [HCO_3^-] + [CO_3^{2-}] \quad (2.14)$$

Where ( ) denotes activity, [ ] denotes molarity and K' equals apparent equilibrium constant after adjustment for Debye – Huckel effects.

When CO_2 is applied to water it transforms to H_2CO_3 as given in Equation 2.15. H_2CO_3 then partly dissociates giving off H^+ to yield HCO_3^- (Equation 2.13), causing a drop in pH.

$$CO_2 + H_2O \Leftrightarrow H_2CO_3 \qquad (2.15)$$

In a mixed sulphide and carbonate system, CO_2 addition, apart from performing the physical role of carrying H_2S bubbles out of the water, shifts the equilibrium of the sulphide system towards the volatile species H_2S. In this regard, a drop in pH to around pH 6 is sufficient since at this pH, over 95% of the sulphide is in the H_2S form.

CHAPTER 3
REMOVAL OF SULPHIDE SPECIES AND ELEMENTAL SULPHUR RECOVERY

3.1 DISCUSSION OF INDUSTRIAL SULPHIDE REMOVAL PROCESSES

A literature survey indicates that a number of approaches exist in practice for the recovery of elemental sulfur by oxidation of sulphide. These can be broadly divided into the following:

a. biologically induced or mediated systems (which are not considered in this contract)
b. Oxidation of gaseous hydrogen sulphide using various gas treatment process
c. Oxidation of aqueous sulphide phase using ferric as the oxidant.

With regard to the gas treatment it would appear that these are the most developed process(es) and arise within the treatment of oil refinery gases. A summary of the various gas treatment processes is given in Table 1. It should be noted that if any of these processes were to be applied to the Rhodes process*, they could only be affected by first stripping the sulphide from the aqueous phase using carbon dioxide. However the sulphide rich waters have a very high proton accepting capacity (i.e. high alkalinity) resulting from the previous sulphate-reducing step. Consequently the effluent will have a high carbon dioxide removal capacity before attaining a pH in which efficient hydrogen sulphide stripping can be affected to reduce S_T to low levels. Efficient scrubbing by carbon dioxide would imply low hydrogen sulphide partial pressure. However the efficiency of many of the gas treatment processes decrease drastically with low hydrogen sulphide partial pressure. These will be costly. A further adverse financial consideration is that all these processes have patent considerations.

With regard to an aqueous phase chemical oxidation process, a literature review indicates that the only viable oxidant in elemental sulphur recovery is ferric. This process utilizes a tubular (silicone) membrane system (ref De Smul). In this process silicone tubes are submerged in a strongly acidic (pH<1.5) ferric sulphate solution. A sulphide-rich solution is pumped through the tubes. $H_2S_{(aq)}$ in the solution diffuses through the pores of the hydrophobic silicone membrane and simultaneously reacts with the ferric to form sulphur.

The authors give rates of H_2S diffusion across the membrane and mention that elemental sulphur form on the silicone tube and falls off with time. However they do not mention the nature of the products produced in the ferric solution. This is an important point because from equilibrium consideration (as discussed early) one would expect sulphate to totally dominate. If elemental sulphur dominates then, the process would appear to be controlled by kinetics. That is, at a pe and pH existing in the ferric solution, the rate of oxidation to elemental sulphur is very much greater than the rate to sulfate, and further, the rate of oxidation of elemental sulphur to sulphate is extremely slow.

In the light of the above, removal of pure sulphide species (excluding metal sulphides) and elemental sulphur recovery were investigated using two approaches: the first as proposed by De Smul and Verstraete (1999) i.e. utilization of a silicone membrane to effect $H_2S_{(g)}$ separation from solution, and the second H_2S stripping using CO_2. With regard to the latter, the kinetics of stripping induced by hydraulic characteristics in the reactor (i.e. the mixing regime that leads to surface area to volume ratio that favours H_2S diffusion) were firstly investigated and a basic model was developed. Thereafter, stripping using an external substance (in this case CO_2) was tested. In this regard the CO_2 acted both as acidic agent to shift the sulphide equilibrium towards H_2S and as a carrier gas for the actual stripping.

In both cases the H_2S gas (after it has been separated from solution) is bubbled into a ferric solution where it oxidizes to elemental sulphur, and settles rapidly.

Experimental results show that the two approaches result in almost complete H_2S removal. However, it will be shown that the kinetics of the silicone membrane process are very slow and as such do not warrant further consideration in the context of AMD treatment. On the other hand, H_2S stripping using CO_2 is a feasible process with favourable kinetics, and its cost effectiveness will largely depend on CO_2 cost.

3.2 SULPHIDE REMOVAL USING SILICONE MEMBRANE

De Smul and Verstraete (1999) showed that silicone tubing is permeable to hydrogen sulphide and used this observation to recover elemental sulphur. This was effected by immersing the silicone tubing conveying the sulphide solution into a high concentration ferric solution.

Ferric ion oxidises the diffused hydrogen sulphide to elemental sulphur (S^0) forming ferrous species. S^0 formed is granular and this makes that it is readily separable. Recovery of ferric from the ferrous species generated must then be effected biologically in a separate reactor to allow for a continuous reaction.

Sulphide removal and sulphate recovery using the "membrane process" is described schematically in Figure 3.1

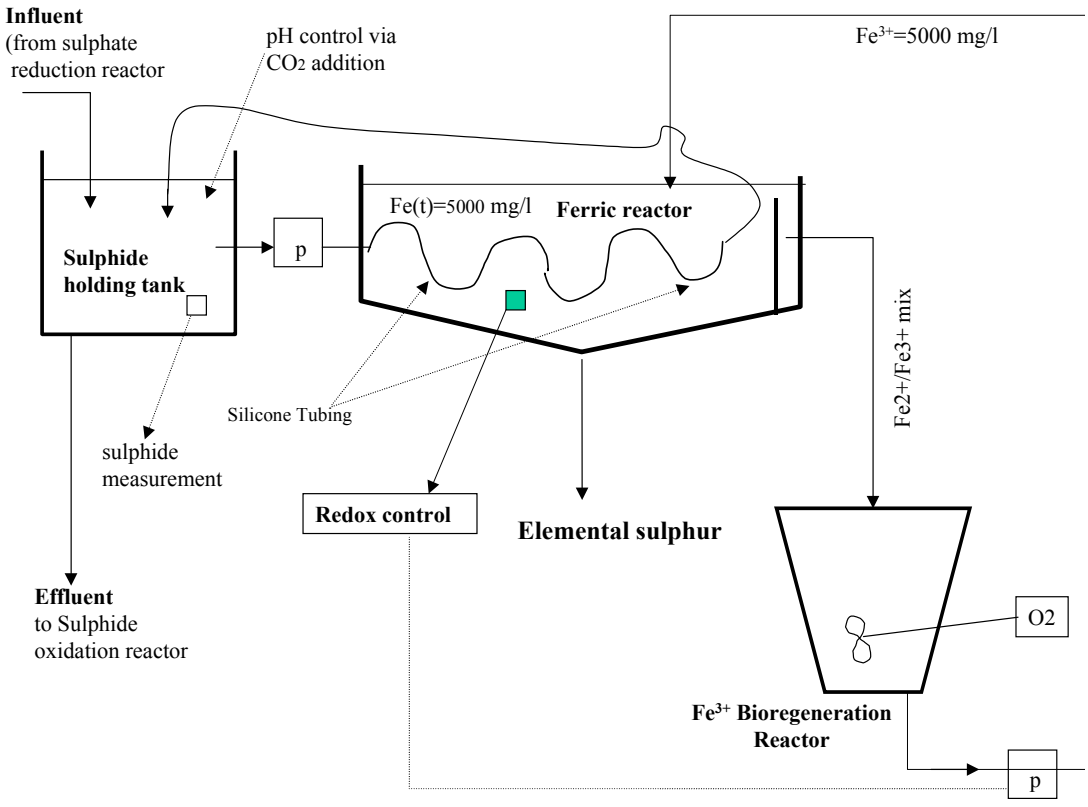

Figure 3.1 The sulphur recovery process

De Smul and Verstraete (1999) showed that H_2S diffusion across the membrane is the rate-limiting step in this S recovery process provided that turbulent flow conditions are maintained for the sulphide solution. Observed kinetics were modelled using a first order rate equation.

This equation can be simplified by recognizing that H_2S alkalinity (proton accepting capacity with reference species H_2S) of the sulphide solution does not change with H_2S addition/removal to yield the following:

$$\frac{S_T}{1+10^{pH-pK_a}} = \frac{S_{T\,(t=0)}}{1+10^{pH_{(t=0)}-pK_a}} \cdot e^{-K'At} \qquad (3.1)$$

Where
S_T - total dissolve sulphide in the bulk of the sulphide solution = $H_2S_{(aq)} + HS^-_{(aq)}$
K' - an experimentally determined rate constant for a particular temperature, tubing wall thickness and dynamics of sulphide fluid flow.
A – total surface area of the tubing (m^2)
t – time in selected units

Equation 3.1 can be used for design purposes once the K' value has been measured.

3.3 EXPERIMENTAL RESULTS

To verify the results obtained by De Smul and Verstraete the experimental set-up given in Figure 3.2 was used. The membrane used was a silicone tube 4 mm in diameter, with wall thickness of 0.7 mm, and length of 4 m. The initial sulphide solution comprised 0.5 litres at a concentration of 500 mg/ℓ. To favour stripping kinetics, the reaction was effected at pH 6, and 1 M HCℓ was used to maintain a constant pH.

Results of the change of sulphide concentration with time and the rate of sulphide passing across the membrane as a function of S_T are shown in Figures 3.3 and 3.4.

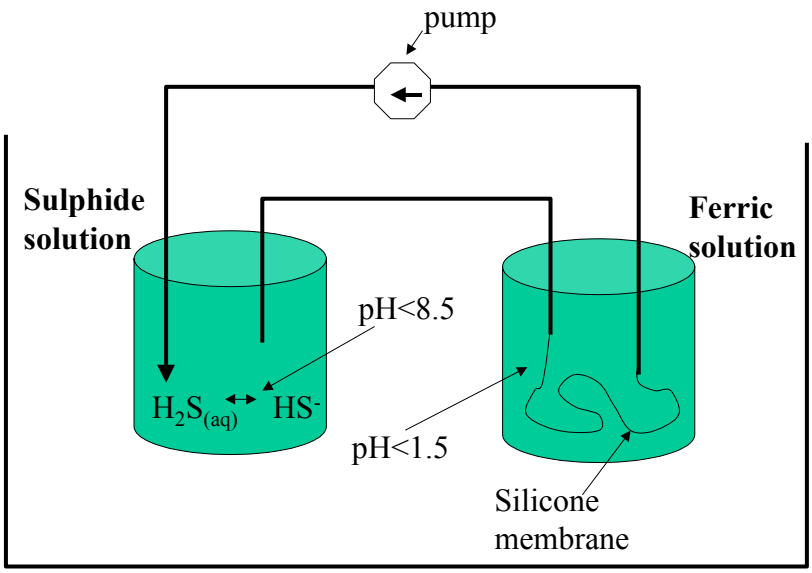

Figure 3.2 Experimental set-up used in this work (after De Smul and Verstraete (1999))

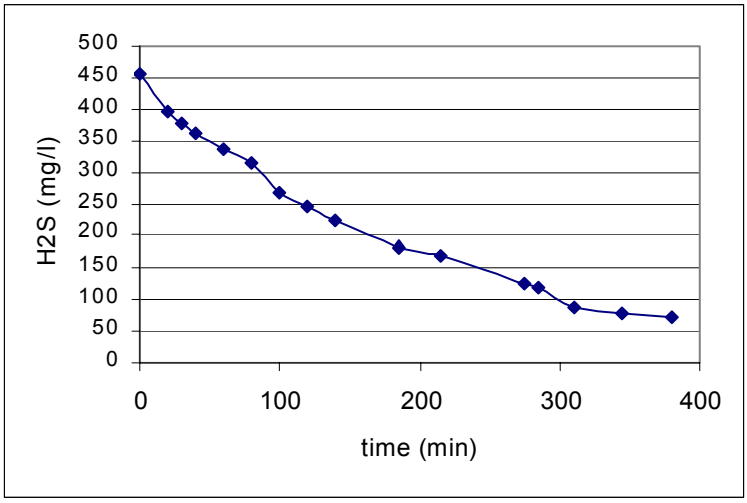

Figure 3.3 Change in sulphide concentration with time using the "membrane process"

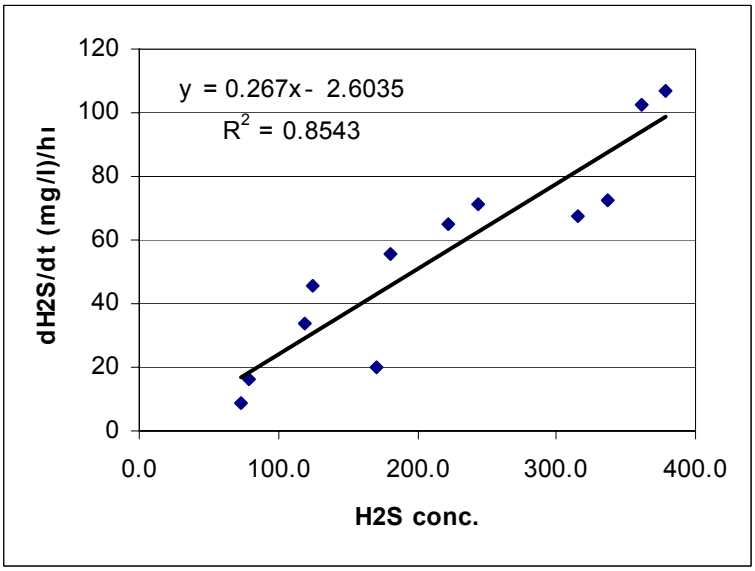

Figure 3.4 Sulphide movement across the membrane as a function of S_T

From the data shown in Figure 3.4 the average rate of sulphide moving across the membrane vs. sulphide concentration was determined and it was found that the membrane process can be used to recover sulphur at a rate of about 140 g S/m^2 tubing surface area/d, using an initial sulphide concentration of around 500 mg S/l at pH=6. It should be noted that these results are valid only for silicone tubing with an internal diameter of 4 mm and a wall thickness of 0.7 mm. This value, which is similar to that reported by De Smul and Verstraete (1999), is unrealistic for a full-scale operation applicable to the large volumes of water to be treated in the AMD scenario.

3.4 SULPHIDE STRIPPING USING CO_2

The second alternative to sulphide removal using physico – chemical methods involved stripping of H_2S using CO_2 gas. In this process the CO_2 has two roles. First, it acts as a source of acidity lowering pH into a region where dissolved H_2S is the dominant species, and second it acts as a carrier gas into which the H_2S diffuses. The CO_2/H_2S gas mixture is then bubbled through a ferric solution resulting in rapid diffusion/oxidation of the hydrogen sulphide component of the carrier gas into solid elemental sulphur granules. The stoichiometry of the process can be depicted as

H_2S stripping

$$HS^- + 2CO_{2(g)} + H_2O \rightarrow H_2S_{(g)} + HCO_3^- + CO_{2(g)} \quad (3.2)$$

Elemental S^0 recovery

$$CO_{2(g)} + H_2S_{(g)} + 2Fe^{3+} \rightarrow 2\ Fe^{2+} + S^0 + 2H^+ + CO_{2(g)} \quad (3.3)$$

Stripping experiments were effected using the setup depicted in Figure 3.5.

Experiments were conducted with three different CO_2 flow rates: 1.85 l/min, 2.5 l/min and 1.2 l/min. Sulphide and ferrous samples were taken with time. From stoichiometry it was expected that the molar increase in ferrous mass closely equalled the decrease in sulphide mass removed. This would assume that no sulphide escapes from the ferric tank, and elemental sulphur is the sole final product (no SO_4^{2-} formation).

3.5 RESULTS

In Figures 3.6 and 3.7 are shown plotted the sulphide and ferrous concentrations with time for the three experiments effected.

As expected, the rates of sulphide stripping and ferrous generation were proportional to the CO_2 flow rate.

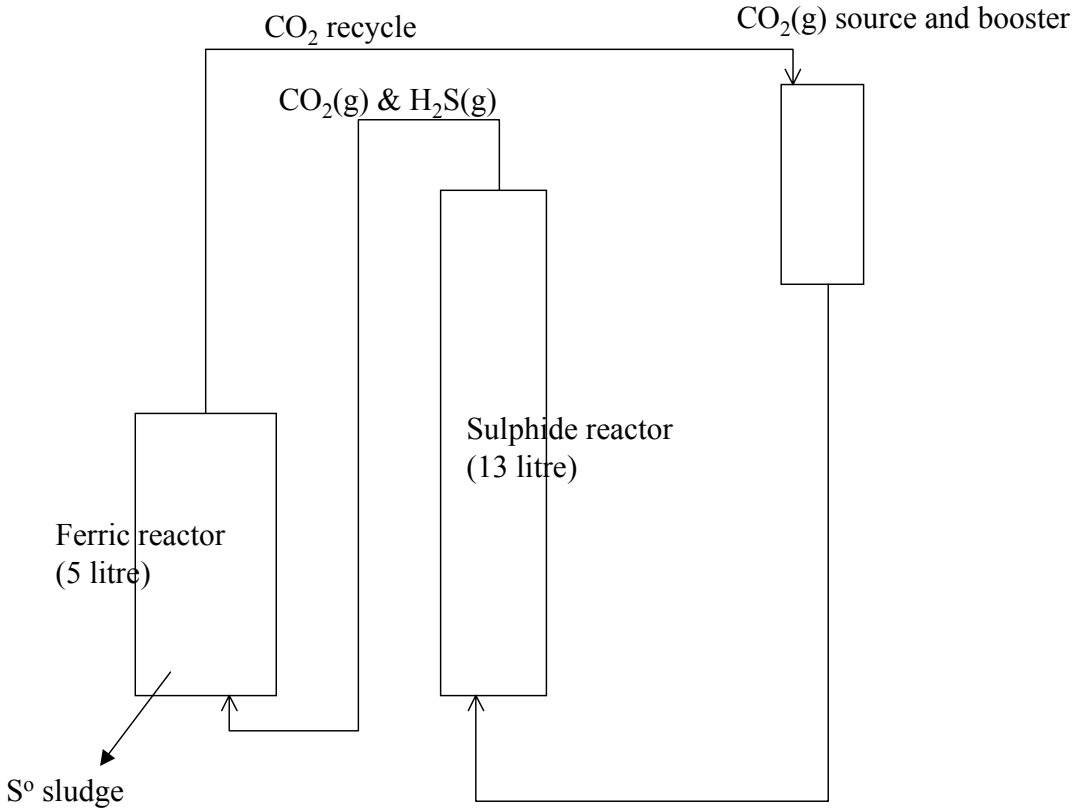

Figure 3.5 Experimental set-up for H_2S stripping experiments

It would appear that for the particular experimental configuration the rate of H_2S stripping followed an equation of the form:

$$\frac{dH_2S}{dt} = KA\left[(H_2S)_l - (H_2S)_g\right] \tag{3.4}$$

Where
K - rate constant for H_2S stripping (l/(m^2 mg))

Since the CO_2 totally dominated the gas phase, the first assumption was to assume that the $(H_2S)_g$ term in the equation be neglected.

The equation, therefore, becomes

$$\frac{dH_2S}{dt} = KA\left[(H_2S)_l\right] \tag{3.5}$$

A plot of ΔH_2S / ΔT vs. H_2S dissolved concentration is shown in Figure 3.8. Referring to Figure 3.8, the slopes of the plots are completely linear and thus give a reasonable estimate of the value of K ∗ A. It would thus appear that the assumption regarding the concentration of $H_2S_{(g)}$ was reasonable.

To determine the rate constant K,, the total surface area of the bubbles, A, needs to be estimated.

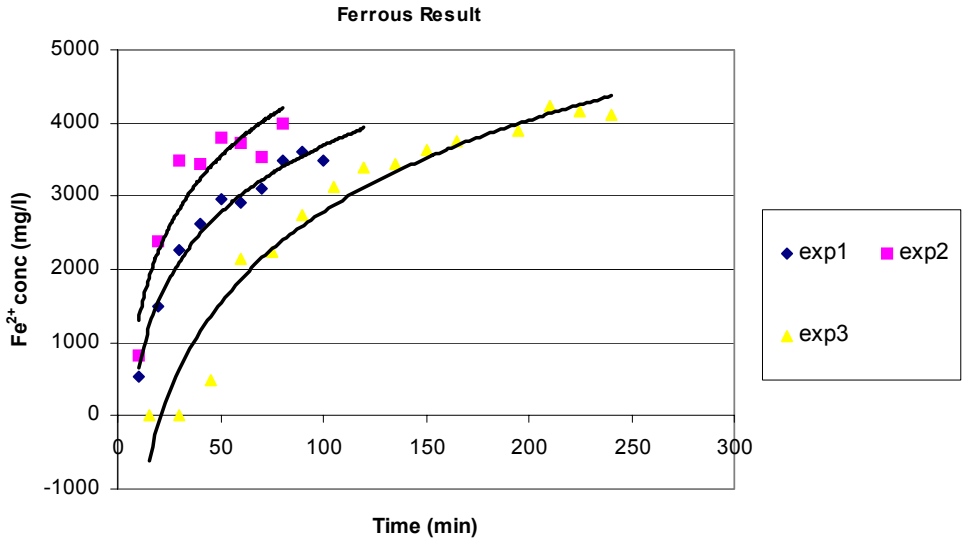

Figure 3.6 Change in ferrous concentration with time for the three experiments

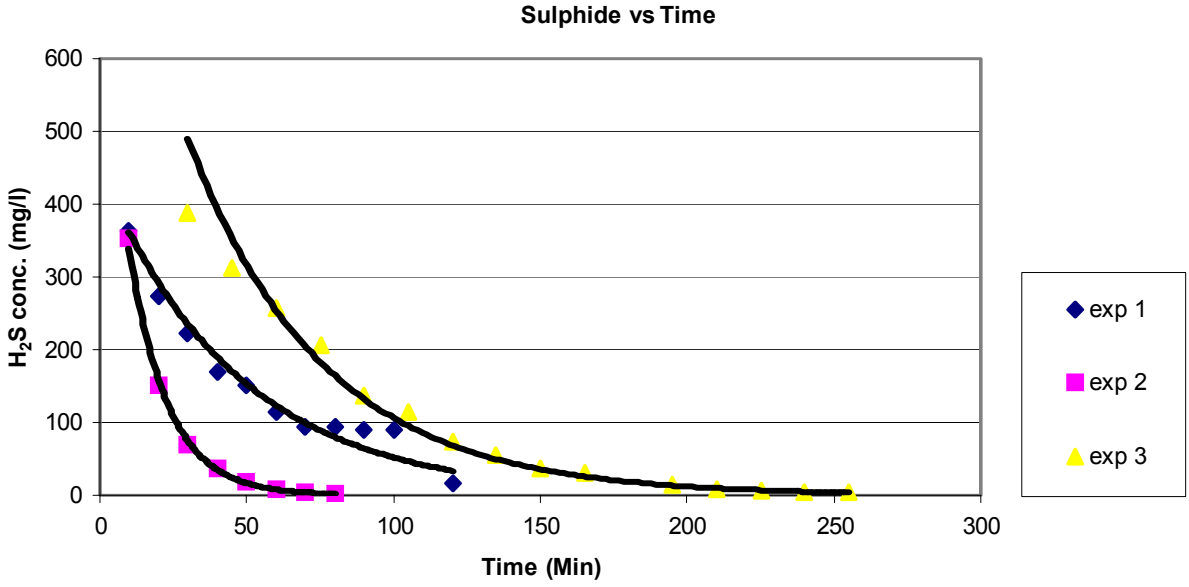

Figure 3.7 Change in sulphide concentration with time for the three experiments

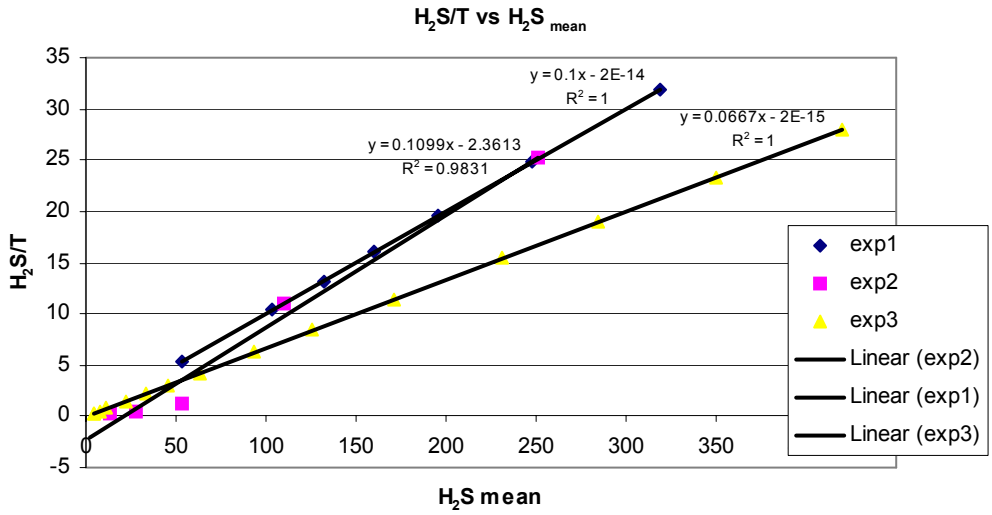

Figure 3.8 Rate of H_2S stripping (in mg S/l/min) versus H_2S concentration (mg/ℓ)

3.6 ESTIMATION OF TOTAL SURFACE AREA OF THE CO_2 BUBBLES

The CO_2 gas flow being diffused into the liquid was measured using a gas flow-meter. Individual mean bubble sizes (in each of the three cases) were estimated visually together with the mean hydraulic retention time (RT_{bubble}) of typical bubbles. From these, the total CO_2 volume in the reactor at any given time V_{CO2} was determined

V_{CO2} (l)= $Q_{CO2} * RT_{bubble}$

The number of bubbles in the reactor at any given time n_{CO2}, was then determined as
$N_{CO2} = V_{CO2} / v_{CO2}$

Where
V_{CO2} = The mean volume of an individual bubble (mℓ).

The total surface area CO_2 in the reactor at any given time (A) (in mm^2) was therefore determined as

$A = n_{CO2} * a_{CO2}$
Where a_{CO2} is the calculated surface area of an individual bubble.

In Table 3.1 are listed the pertinent data for the three experiments and the respective calculated $CO_{2(g)}$ total surface areas.

3.7 DETERMINATION OF K – RATE CONSTANT FOR H_2S STRIPPING

Having calculated the total CO_2 surface area, and having determined the slopes from Figure 3.8, the rate constant K can be determined. The relevant data is given in Table 3.2 for the three experiments.

Referring to Table 3.2, the rate constant for the three experiments is closely equal. The average value of K obtained was 3.15*10-7 accompanied with a standard deviation of $14.15*10^{-7}$ l/mg/m^2.

This observation gives credence that the rather crude methodology employed was adequate.

Table 3.1 Data and calculations of total surface area of bubbles

Parameter		Exp1	Exp2	Exp3
Flow rate	(l/min)	1.85	2.5	1.2
Mean bubble diameter	(mm)	4	4.5	0.5 – 5
Retention time of gas in reactor	(min)	0.1	0.098	0.103
Volume of gas in reactor	(mm^3)	185000	245833	124000
Volume of single bubble	(mm^3)	33.5	47.7	33.5
No. of bubbles		5520	5152	3700
Surface area of a single bubble	(mm^2)	50.2	63.6	50.2
Total area	(mm^2)	277500	327777	186000

Table 3.2 Determination of K - rate constant for H_2S stripping

Experiment	**Mean $\Delta H_2S/\Delta T$**	**S stripping rate**	**Area of Bubble**	**K (constant)**
		1/(min)	(mm^2)	1/(min*mm^2)
1	14.88216	0.1	277500	$3.6\ 10^{-7}$
2	6.620144357	0.1099	327777.7778	$3.3\ 10^{-7}$
3	8.304576042	0.0667	186000	$3.58\ 10^{-7}$

3.8 CONCLUSIONS

a. Sulphide stripping using silicone membranes: the tentative experiments conducted here would indicate that removal of sulphide via H_2S moving across a silicone membrane allows S^0 removal at about a rate of 140 g S^0 / m^2 membrane per day for a membrane thickness of 0.7 mm. This rate is too low to have practical viability for treatment of large volumes of water such as AMD effluents. Furthermore, the possibility of membrane fouling due to biological activity or mineral precipitation will further reduce this rate and the feasibility of this approach.

b. H_2S stripping using CO_2 and sulphur recovery using ferric as oxidant appears to have kinetics that would allow the process the be employed in the treatment of large volumes of biologically reduced AMD effluents. However, there is a high cost

associated with CO_2 being lost due to dissolution into the AMD water for pH adjustment. This loss of CO_2, on a volumetric basis, closely equals the sulphide being stripped assuming a low buffer capacity of the AMD water. Clearly, a fraction of the CO2 (> 95%) is continuously recycled.

REFERENCES TO CHAPTER 3

CARROL, J J, Reliability Prediction of the Solubility of H_2S in Water. Chemical Engineering, October 1990.

D"YACHKOVA, I B and KHODAKOVSKIY, I L, Thermodynamic Equilibrium in the Systems S-H_2O, Se-H_2S, and Te-H_2 in the 25-300^oC Temperature Range and Their Geochemical Interpretations. Geokhimiya, No. **11**, pp. 1358-1375, 1968.

GARRELS, R M and NAESER, C R, Equilibrium Distribution of Dissolved Sulphur Species in Water at 25^oC and 1 atm total Pressure, Geochimica et Cosmochimica Acta, 1958, Vol. **15**, pp. 113 – 130.

HARDISON, L C, Go from H_2S to S in one unit, Hydrocarbon Processing, April 1985, pp 70-71.

HARDISON, L C and RAMSHAW, D E, H_2S to S: process improved, Hydrocarbon Processing, January 1992, pp 89-90.

HEISEL, M P and MAROLD F J, New Gas Scrubber Removes H_2S, Hydrocarbon Processing, April 1987, pp. 34-37.

JENSEN, A B and WEBB, C, Treatment of H_2S-containing gases: A Review of Microbiological Alternatives, Enzyme and Microbial Technology, May 12, pp. 2-10.

JOHNSON, J E, Options narrowed to Claus or Process Processes, Oil & Gas Journal, November 22, pp. 70-76.

MILLERO, F J, The Thermodynamics and Kinetics of the Hydrogen Sulphide System in Natural Waters. Mar. Chem., 1986, **18**: 121 –147.

RAO, R S and HEPLER, L G, Equilibrium Constants and Thermodynamics of Ionization of Aqueous Hydrogen Sulfide. Hydrometallurgy, **2** (1976/1977), pp. 293-299.

SNEED, M C and MAYNARD, J L, General Inorganic Chemistry. 3rd edition,1942, New York.

STUMM, W and MORGAN, J J, Aquatic Chemistry: An Introduction Emphasizing Chemical Equilibria in Natural Waters. John Wiley & Sons, Inc, 1970.

SULEIMENOV, O M and KRUPP, R E, Solubility of Hydrogen Sulfide in Pure Water and in NaCl Solutions, from 20 to 320^oC and at Saturation pressures. Geochimica et Cosmochimica Acta, 1994, Vol. **58**, No. 11, pp. 2433– 2444.

CHAPTER 4

COAGULATION/FLOCCULATION OF METAL IONS IN THE CONTEXT OF THE RHODES PROCESS

4.1 INTRODUCTION

In the conceptualisation of the Rhodes Process the recycle of sulphide-rich treated waters would promote for the precipitation of metals present in AMD as metal sulphides, and possibly also metal carbonates. Preliminary studies had indicated the feasibility of this as a unit operation in the overall process. However, this unit process was not investigated in the pilot plant to any further extent due to time constraints. This resulted in a more intensive laboratory scale investigation into the feasibility of the metal ion precipitation/coagulation/ flocculation process. These investigations are reported in this chapter after first dealing with theoretical aspects of the aqueous chemistry involved.

4.2 BASIC CHEMISTRY OF ACID MINE DRAINAGE WATERS

With regard to the chemistry of the blended water resulting from a mix of high-sulphide process recycle water and the raw untreated AMD waters, successful precipitation of the metals will depend on a number of factors including: pH; sulphide concentration and metal ion concentration of the blend.

pH established will depend principally on two factors: firstly, aqueous phase weak acid/base considerations that is, on the alkalinity and acidity of the blend; secondly, on the molar masses of metal sulphide (and metal carbonates) that precipitate. Such precipitation removes S^{2-} species and perhaps CO_3^{2-} and OH^- species thereby reducing alkalinity and pH. These effects can be explained in terms of equilibrium chemistry.

Aqueous phase equilibrium

The blended water contains three weak acid base systems and these in turn govern pH. The three systems are the sulphide system (H_2S, HS^-, and S^{2-} species); carbonate systems (H_2CO_3, HCO_3^- and CO_3^{2-} species) and the water system itself (H^+ and OH^- species). Aqueous phase equilibrium equation relationships for each of these systems are set out below. System mass and capacity equations are then formulated.

Sulphide system

Gives us the concomitant equilibrium equation

$$\frac{(H^+)(HS^-)}{(H_2S)} = K_{s1} \qquad (4.1)$$

($pK_1 = 7.06$ at 20^0C) and

$HS^- \leftrightarrow H^+$ and S^{2-}

Giving

$$\frac{(H^+)(S^{2-})}{(HS^-)} = K_{s2} \quad (4.2)$$

Where $pK_2 = 13.89$ at 20^0C

With regard to pH buffering, equation 2 above can be ignored because pH of the AMD/high sulphide blend is pH of ≈ 6.8, which is very far away from the pKa of 13 and S^{2-} species concentration is negligible.

Carbonate system
A similar set of weak acid equilibrium equations as set out above for the sulphide system can be formulated for the carbonate system

$$\frac{(H^+)(HCO_3^-)}{(H_2CO_3)*} = K_{c1} \quad (4.3)$$

Where $(H_2CO_3)^*$ = sum of CO_2 dissolved and $H_2CO_3^-$ and $pK_{c1} = 6.38$

$$\frac{(H^+)(CO_3^{2-})}{(HCO_3^-)} = K_{c21} \quad (4.4)$$

Where $pK_{c2} = 10.32$

Water system
The single equilibrium equation

$(H^+)(OH^-) = K_w$

Capacity equations for the system are formulated as the proton accepting (alkalinity) and donating (acidity) capacities with respect to selected reference species. For alkalinity, selecting the most protonated species (i.e. $H_2CO_3^*$ and H_2S) and pure water as reference species

$$\text{Alkalinity} = 2[CO_3^{2-}] + [HCO_3^-] + 2[S^{2-}] + [HS^-] + [OH^-] - [H^+] \quad (4.5)$$

Where [ ] = molaraties.

In the pH region of the blended water (pH≈ 6.8) the alkalinity equation simplifies to

$$\text{Alkalinity} = [HCO_3^-] + [HS^-] \quad (4.6)$$

For acidity, selecting the least protonated species (CO_3^{2-} and S^{2-}) and pure water as reference species:

$$\text{Acidity} = 2[H_2CO_3]^* + [HCO_3^-] + 2[H_2S] + [HS^-] + [H^+] - [OH^-] \quad (4.7)$$

And the pH region under consideration this approximates to

$$\text{Acidity} = 2[H_2CO_3]^* + [HCO_3^-] + 2[H_2S] + [HS^-] \quad (4.8)$$

The system mass parameters are simply the sums of the individual species comprising each weak acid base sub-system. For the carbonate system, the total dissolved carbonate system, the total dissolved carbonate species dissolved in solution (C_T) is given by

$$C_T = [H_2CO_3] + [HCO_3^-] + [CO_3^{2-}] \quad (4.9)$$

And for the sulphide system (S_T), total dissolved sulphide species by

$$S_T = [H_2S] + [HS^-] + [S^{2-}] \quad (4.10)$$

In order to characterize the aqueous phase, one parameter needs to be known for each of the three sub-systems: carbonate, sulphide and pure water. That is, if S_T, C_T and pH are known, each of the weak acid species concentration in solution can be determined using the above set of equations. This becomes important when determining the saturation state of the solution with respect to certain minerals which may precipitate.

Aqueous solid phase equilibrium

Various carbonate, sulphide and hydroxide species may precipitate when the recycled sulphide-rich high pH water is blended with incoming raw AMD water. For the Fe^{3+} species in the pH region of the blend, the Fe^{3+} concentration will be controlled by $Fe(OH)_3$ mineral or sulphated ferric hydroxide (jarosite) (Schwertman and Fechter., 1994; Drissi et al., 1995) i.e.

$$(Fe)(OH)_3 = K_{sp} \quad (4.11)$$

Where $K_{sp} = 10^{-37.5}$

For the Fe^{2+} species any one or all of hydroxide, sulphide and/or carbonates may precipitate.

For $Fe(OH)_2$

$$(Fe)(OH)_2 = K_{sp} \quad (4.12)$$

Where $K_{sp} = 14.7$

For ferrous carbonate (siderite)

$$(Fe^{2+})(CO_3^{2-}) = K_{sp} \quad (4.13)$$

Where $K_{sp} = 10.7$

For Ferrous sulphide, this is commonly given in terms of the HS^- concentration, i.e. the equilibrium reaction

$$FeS + H^+ \leftrightarrow Fe^{2+} + HS^- \quad (4.14)$$

This leads to the solubility product

$$\frac{(Fe^{2+})(HS^{-})}{(H^{+})} = pK$$

Where $K_{sp} = 4.10^{-19}$

In general, the remaining heavy metal ions will be present at lower concentrations relative to the iron species, the metal sulphide will dictate the concentration of these species in solution.

In addition to the above precipitants that occur in the region ≈pH7 it was found that if the blend pH is artificially lifted to pH 8 and greater, green rust (II), a Fe^{2+}/Fe^{3+} sulphated hydroxide also precipitates. The importance of this mineral precipitate is similar to that of $Fe(OH)_3$, that is it forms flocculent precipitates that effect good removal of the colloidal metal sulphide precipitants (Bessiere et al.,1999).

Laboratory-scale investigations were initiated in order to assess the metal removal using the proposed Rhodes BioSURE process. While this proved disappointing a further investigation was undertaken to investigate the feasibility of operating at a higher pH using lime at the blending point. These investigations are reported below with principle objectives being to investigate

i. metal sulphide precipitation using sulphide-rich overflow liquor from biological sulphate reducing digesters fed on a complex carbon source, namely primary sewage sludge,
ii. the coagulant properties of ferric ions with regard to destabilizing the FeS and metal sulphide colloidal suspensions at various ratios,
iii. the effects of lime dosage on enhancing metal removal,
iv. the effects of varying the sulphide concentration have on metal-sulphide precipitation.

4.3 RESULTS AND DISCUSSION

Simulation of iron removal in the Rhodes BioSURE process

In the pilot plant studies iron removal (and other metal ions) was effected by establishing a blend of sulphide-rich process recycle water with incoming raw AMD waters, such that the ratio of sulphide to total iron in the blend was stoichiometric (on the molar scale 1:1). It should be noted that in the preliminary pilot plant investigation the Fe^{3+} component of the total iron was not measured. Recognising that ferric sulphide does not precipitate, the sulphide: Fe^{2+} ratio was, therefore, some value in excess of unity. However, the Fe^{3+} species present should form $Fe(OH)_3$ with excellent coagulation/flocculation properties.

Table 4.1 lists the results of laboratory-scale experiments using various Fe^{3+} iron concentrations in order to assess the effects of Fe^{3+}/Fe^{2+} ratio on iron removal. The concentration of Fe^{3+} ranged from 10 –70% of the total iron available in the experiment. It should be noted that the iron remaining, i.e. Fe(t)(f) is composed of both dissolved and colloidal (suspended) iron species.

In Figure 4.1 shown plotted is the residual iron remaining versus Fe^{3+} added. The plot shows a decrease in non-settlable iron remaining with increase in percent Fe^{3+}. Generally the experiments indicate poor iron removal. The best result being residual Fe total content of ≈ 90mg/l (at pH 6.5 investigated) was with 70 percent Fe^{3+} added.

Table 4.1 Laboratory-scale simulation of iron removal from acid mine drainage wastewaters

Exp. No	**% Fe^{3+} of Fe(t)(i)**	**Ratio Fe^{2+}(t)(i):S^{2-} (t)**	**pH(i)**	**pH(f)**	**Fe(t)(i)**	**Fe(t)(f)**
1	10	1 to 1	6.56	6.37	200 mg/l	159 mg/l
2	20	1 to 1	6.51	6.41	214 mg/l	104 mg/l
3	20	1 to 1	6.45	6.33	207 mg/l	132 mg/l
4	30	1 to 1	6.57	6.4	208 mg/l	123 mg/l
5	37	1 to 1	6.54	6.23	223 mg/l	131 mg/l
6	39	1 to 1	6.56	6.4	213 mg/l	119 mg/l
7	40	1 to 1	6.51	6.38	199 mg/l	109 mg/l
8	43.8	1 to 1	6.54	6.39	199 mg/l	91 mg/l
9	50	1to 1	6.49	6.37	199 mg/l	86 mg/l
10	60	1 to 1	6.53	6.46	199 mg/l	77 mg/l
11	70	1 to 1	6.46	6.3	199 mg/l	93 mg/l
12	70	1 to 1	6.53	6.4	199 mg/l	82 mg/l

(i) = initial, **(f)** = final and **(t)** = total concentration

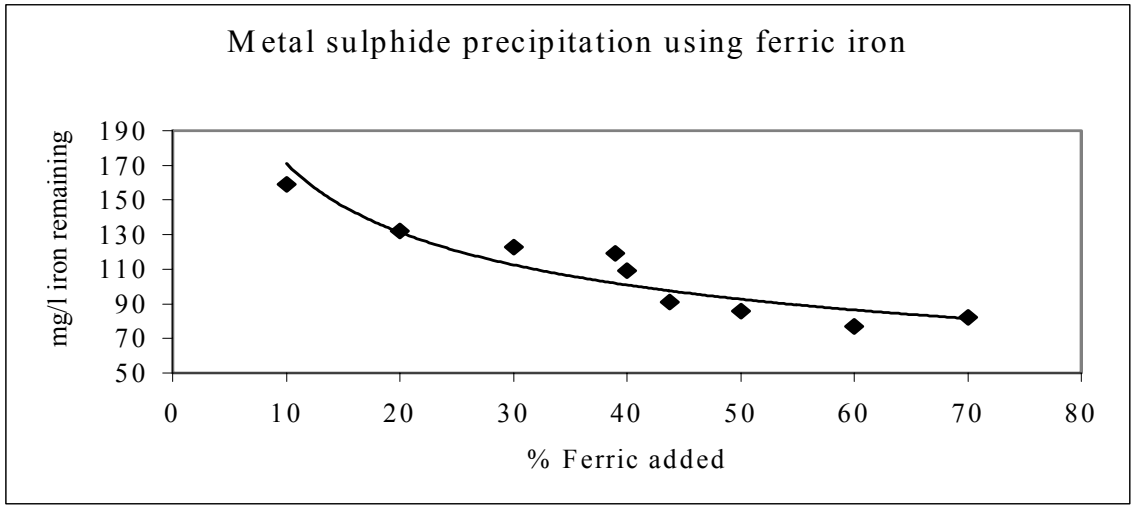

Figure 4.1 Observations on the effects of increased Fe^{3+} and showing the residual iron concentration remaining in solution for solutions with ferrous to sulphide ratios (molar scale) of unity

The poor results obtained perhaps reflects that the Fe^{3+} did not all precipitate as $Fe(OH)_3$, and that the sulphide species did not all precipitate as metal sulphides. Most likely some of the sulphide species were oxidised to elemental sulphur. The electron acceptor in the oxidation process would be Fe^{3+} species being reduced to the Fe^{2+} species, i.e.

$$HS^- \rightarrow S^o + H^+ + 2e \quad (4.15)$$
$$2Fe^{3+} + 2e^- \rightarrow 2Fe^{2+} \quad (4.16)$$

Giving the resultant redox reduction

$$HS^- + 2Fe^{3+} \rightarrow S^o + 2Fe^{2+} + H^+ \quad (4.17)$$

This reaction is extremely fast and forms the basis for sulphide removal in the oil refinery industry.

The effects of such a redox reaction would be a Fe^{2+}: sulphide ratio that is very much greater than unity (leaving a residual Fe^{2+} in solution). Furthermore, the Fe^{3+} species would be reduced, thereby impairing the good coagulating properties. The resultant effect is the ineffective removal of metal sulphide colloids (Table 4.2). If this hypothesis is correct some modification to the existing process needs to be made.

Table 4.2 Laboratory-scale simulation of iron removal from acid mine drainage wastewaters with the Fe^{II}/S_{Total} ratio being altered

Exp. No	PH(i)	pH(f)	Fe(t)(i)	Fe(t)(f)	%Fe^{3+} of Fe(t)(i)	Ratio Fe^{2+}(t)(i): S^{2-}(t)
1	6.53	6.42	200mg/l	89mg/l	60	1 to 1.3
2	6.49	6.39	200mg/l	86mg/l	60	1 to 1.3
3	6.48	6.39	200mg/l	137mg/l	30	1 to1.5
4	6.47	6.37	200mg/l	141mg/l	30	1 to1.5

(i) = initial, **(f)** = final and **(t)** = total species concentration

Simulation of iron removal with addition of lime

The poor results obtained from the blending of a sulphide-rich process recycle with influent, required that further investigations should be effected to obtain acceptable metal removal. In this regard it was found, at laboratory-scale, that an increase in pH (≥ 7.8) using lime resulted in a thick green precipitate being formed. This occurred provided that, either or both the ferric component to total iron was in the region of 10-20 percent and/or the untreated water contained more than 3mg/l dissolved oxygen. The settling characteristics of this floc were excellent. A literature review into processes involving metal removal at this elevated pH gave no indication as to the nature of the precipitants involved. A more recent review involving current fundamental chemistry research into the iron system indicates that the flocculant precipitate is green rust (II), a Fe^{3+}/Fe^{2+} sulphated hydroxide ($Fe_2^{III}\ Fe_4^{II}\ SO_4(OH)_{12}$) (Lowe et al., 1988).

The formation of green rust II under these conditions is hypothesised to follow reaction (1) and perhaps either or both of equations 4.19 and 4.20:

$$6Fe(OH)_2 + SO_4^{2-} + \tfrac{1}{2}\ 0_2 + 2H^+ \leftrightarrow Fe_2^{III}\ Fe_4^{II}\ SO_4(OH)_{12} + H_20 \qquad (4.18)$$

$$4Fe(OH)_2 + 2Fe^{3+} + SO_4^{2-} + 4OH^- \leftrightarrow Fe_2^{III}\ Fe_4^{II}\ SO_4(OH)_{12} \qquad (4.19)$$

$$6Fe(OH)_2 + 2Fe^{3+} + SO_4^{2-} \leftrightarrow Fe_2^{III}\ Fe_4^{II}\ SO_4(OH)_{12} + 2Fe^{2+} \qquad (4.20)$$

Over and above green rust II, precipitant, one may also expect co-precipitation of $Fe(OH)_3$ (Jarosite) and $Fe(OH)_2$ (part of which is transformed to green rust II as depicted in reaction (1)) (Schwertman and Fechter, 1994). The fractions of the various precipitants depend on the concentrations of Fe^{2+}, Fe^{3+}, O_2 and SO_4^2 in the AMD waters. These precipitants are labile intermediates in the formation of goethite, lepidocrocite (FeOOH) and magnetite (Fe_3O_4). However the transformation of the fresh green rust precipitate to the stable end products is relatively slow from a process point of view (> 6 hours) and requires an internal electron acceptor (Genin, 1999).

Although the occurrence of the mineral green rust (II) has been shown to occur using various crystallographic techniques (Lowe et al., 1988; Lowe and Genin, 1991; Schwertman and Fechter, 1994), the authors do not give solubility product data. Consequently it was not possible to formulate a quantitative model for the removal of metals. Therefore an empirical

approach has been adopted via treatment of simulated AMD waters blended with a sulphide-rich process recycle stream and an elevated pH.

Considering treatment of the AMD high-sulphide blend at elevated pH, it is important to note that various metal hydroxides and carbonates are also likely to precipitate in addition to the metal sulphides and green rust (II). Again no attempt at mathematical modelling was attempted because this would be meaningless without incorporating the green rust component. However, one is still able to assess the efficacy of metal iron removal from measurements on laboratory-scale tests.

In order to investigate the efficacy with which the green rust (II) precipitant is capable of removing metal sulphide colloids, a number of experiments were effected and the results are reported below

The first set of experiments was set up to enquire into the removal of FeS colloids, and a second set that considers iron $Mn(Cl)_2$ and $Zn(Cl)_2$ removal.

Iron sulphide colloid removal

In Table 4.3 below, are listed the results of an investigation into iron sulphide colloid removal. At 'high' pH in each experiment a colloidal FeS precipitation occurred. Flocculation occurred during a slow-mix period and excellent settling was attained. In all cases the final iron content was undetectable reflecting excellent removal of the FeS (this quantifies the visual observation, which was a relatively clear supernatant). However from a visual point of view the 20 percent initial Fe^{3+} solution gave a clearer solution.

Table 4.3 Iron sulphide colloid removal at high pH with varying ferric concentrations and ferrous to sulphide ratio in laboratory-scale experiments

Exp. No	pH(i)	pH(f)	Fe^{2+}(i)(t)	Fe(t)(f)	%Fe^{3+} of Fe (t)(i)	Ratio Fe^{2+}(t)(i) :S^{2-}(t)
1	6.2	8.2	200mg/l	<5mg/l	10	1 to 1
2	6.19	8.17	200mg/l	<5mg/l	10	1 to 0.5
3	6.17	8.27	200mg/l	<5mg/l	20	1 to 1
4	6.21	8.13	200mg/l	<5mg/l	20	1 to 0.5

(i) = initial, **(f)** = final and **(t)** = total species concentration

Metal sulphide removal

In Table 4.4 below, are listed results of an investigation into the removal of the metal irons: iron, manganese and zinc from simulated Grootvlei AMD waters. In all experiments the Fe^{3+} component of the initial total iron (Fe(i)(t)) was 20 percent, as it was felt that this reflected most closely the real world in situ situation. The initial concentration of ferrous, zinc and manganese were 200mg/l, 2mg/l and 10mg/l respectively. The molar ratio of ferrous to total sulphide (Fe^{2+}(t): S^{2-} (t)) was varied between 1:1; 1:0.5; and 1:0.25.

Lime was added in a rapid mix phase for approximately 20 seconds, and thereafter flocculation was attained under a slow mix period (20 minutes). In all cases, excellent

flocculation and coagulation occurred and fast-settling sludges resulted. The supernatant was sampled for analysis after 30 minutes of settling.

Referring to Table 4.4, in all cases iron was removed to a non-detectable level; for the zinc and manganese species significantly better removal was obtained at the higher total sulphide value. Recognising that all waters were treated to approximately the same pH and had the same initial total carbonate species concentration, one may conclude that metal sulphide precipitation was responsible for this improvement and not metal carbonate or hydroxide precipitation. Furthermore, it is important to note that the improvement in removal zinc and manganese as sulphides was effected even though there was high mineral precipitation competition with ferrous sulphide.

Table 4.4 Metal sulphide colloid removal at high pH with ferric concentration at 20% and varying ferrous to sulphide ratio in laboratory-scale experiments

Exp. No	**pH(i)**	**pH(f)**	**Fe(i)(t)**	**Fe(t)(f)**	**%Fe^{3+} of Fe(t)(i)**	**Ratio Fe^{2+}(t): S^{2-}(t)**	**Zn(i)**	**Mn(i)**	**Zn(f)**	**Mn(f)**
1	6.15	8.22	200mg/l	<5mg/l	20	1 to 1	2mg/l	10mg/l	0.03mg/l	1.46mg/l
2	6.16	8.27	200mg/l	<5mg/l	20	1 to 0.5	2mg/l	10mg/l	0.11mg/l	2.16mg/l
3	6.11	8.17	200mg/l	<5mg/l	20	1 to 0.25	2mg/l	10mg/l	0.21mg/l	2.18mg/l

i) = initial, **(f)** = final, **(t)** = total species concentration

4.4 CONCLUSIONS

A number of conclusions maybe drawn from these studies:

i. In practice AMD waters contain iron species in both Fe^{2+} and Fe^{3+} forms.
ii. Blending untreated AMD waters with sulphide recycle water results in flocculation caused by $Fe(OH)_3$ precipitation at ≈ pH 6.8. The effluent however is turbid with relatively high iron content probably arising from colloidal FeS.
iii. The blending of untreated AMD waters with sulphide recycle probably causes oxidation of sulphide to elemental sulphur with Fe^{3+} acting as electron acceptor forming Fe^{2+} species. The elemental sulphur increases turbidity. More important however, reduction of the Fe^{3+} to Fe^{2+} reduces the coagulation/flocculation efficacy of the Fe^{3+} in the untreated water.
iv. Raising pH of the sulphide AMD blend to pH>8 results in excellent iron removal with a clear supernatant. This probably results from the coagulating properties of green rust (II) ($Fe_2^{III}Fe_4^{II}SO_4(OH)_{12}$) which coagulates iron sulphide colloids.
v. Ninety percent of manganese and zinc were removed from the supernatant at the operational pH and the resultant colloids probably were flocculated by the green rust (II) precipitation.

CHAPTER 5

IRON AND HEAVY METALS IN ACID MINE DRAINAGE WATERS – EQUILIBRIUM AND TREATMENT CONSIDERATIONS

5.1 INTRODUCTION

Acid mine drainage (AMD) waters are acidic with unacceptably high concentrations of *inter alia* iron, heavy metals and sulphates. In the treatment of AMD iron and heavy metals may be precipitated as hydroxides/oxides, carbonates (rarely), sulphides and sometimes sulphates.

The species that precipitate in any scenario will depend on the nature and concentrations of precipitation ions and *inter alia* on pH, redox potential and rates of chemical addition (i.e. mixing configuration).

In this chapter some aspects of hydroxide/oxide and sulphide mineral precipitation are considered with the emphasis on a didactic use of equilibrium chemistry and practical aspects of such precipitation on the treatment of AMD waters.

The chapter is presented by considering first metal hydroxides, then the sulphides and finally metal oxides. In each, aqueous phase and aqueous-solid phase equilibrium form the main thrust and treatment considerations are drawn from these.

5.2 METAL HYDROXIDES

Aqueous phase considerations

All the metals encountered in AMD waters form complexes (and/or ion pairs) with hydroxide species. Such complexing affects the solubility of the mineral as will be shown later. Considering the generic divalent metal ion M^{2+}, up to three hydroxide complexes have been noted i.e. MOH^-, $M(OH)_2^0$, and $M(OH)_3^-$. Though the first (MOH^-) has meaning considering the aqueous phase alone, the remaining two only have significance in determining metal ion solubility (i.e. two phase diagram). Equilibrium constants for these latter complexes were determined from two-phase equilibrium considerations. In Table 1 below are listed data reported for various M^{2+}-hydroxide complexes.

Table 5.1 log of dissociation constants for various divalent metal hydroxides complexes^

Metal ion	***Complex***	***Log dissociation constant****
Fe^{2+}	$Fe(OH)^{+}$	*-4,5*
	$Fe(OH)_2^0$	-7,4
	$Fe(OH)_3^-$	-11,0
Mn^{2+}	$Mn(OH)^{+}$	*-3,4*
	$Mn(OH)_2^0$	-5,8
	$Mn(OH)_3^-$	-7,2
Zn^{2+}	$Zn(OH)^{+}$	*-5,0*
	$Zn(OH)_2^0$	-11,1
	$Zn(OH)_3^-$	-13,6
Ni^{2+}	$Ni(OH)^{+}$	*-4,1*
	$Ni(OH)_2^0$	-9,0
	$Ni(OH)_3^-$	-12,0
Pb^{2+}	$Pb(OH)^{+}$	*-6,3*
	$Pb(OH)_2^0$	-10,9
	$Pb(OH)_3^-$	-12,0

** dissociation reaction $MOH \Leftrightarrow M^{2+} + OH^-$*
^ Source: Stumm and Morgan (1996)

The relevant generic reactions and equations for aqueous phase equilibrium are thus

$$MOH^+ \Leftrightarrow M^{2+} + OH^- \quad (5.1)$$
$$M(OH)_2^0 \Leftrightarrow M^{2+} + 2OH^- \quad (5.2)$$
$$M(OH)_3 \Leftrightarrow M^{2+} + 3OH^- \quad (5.3)$$

For each of these reactions there is a corresponding equilibrium equation

$$[M^{2+}]\,[OH^-] / [MOH^+] = K_{b1}' \quad (5.4)$$
$$[M^{2+}]\,[OH^-]^2 / [M(OH)_2] = K_{b2}' \quad (5.5)$$
$$[M^{2+}]\,[OH^-]^3 / [M(OH)_3^-] = K_{b3}' \quad (5.6)$$

Where K' = apparent equilibrium constant including Debye Huckel effects.

In the practical scenario, the dependant variable of interest is pH and the equilibrium equations should be transformed into this form. Recognizing that water is the solvent, Equation 5.4 becomes.

$$\{[M^{2+}]\,K_w\} / \{[MOH^+]\,[H^+]\} = K_{b1}' \quad (5.7)$$
and
$$[MOH^+]\,[H^+] / [M^{2+}] = K_w/K_{b1}' = K_{a1}' \quad (5.8)$$

Such transformation allows presentation of aqueous phase equilibrium. For example, in Figure 5.1 for the divalent iron hydroxide system with Fe_T (total dissolved ferrous) of $2 * 10^{-2}$ M.

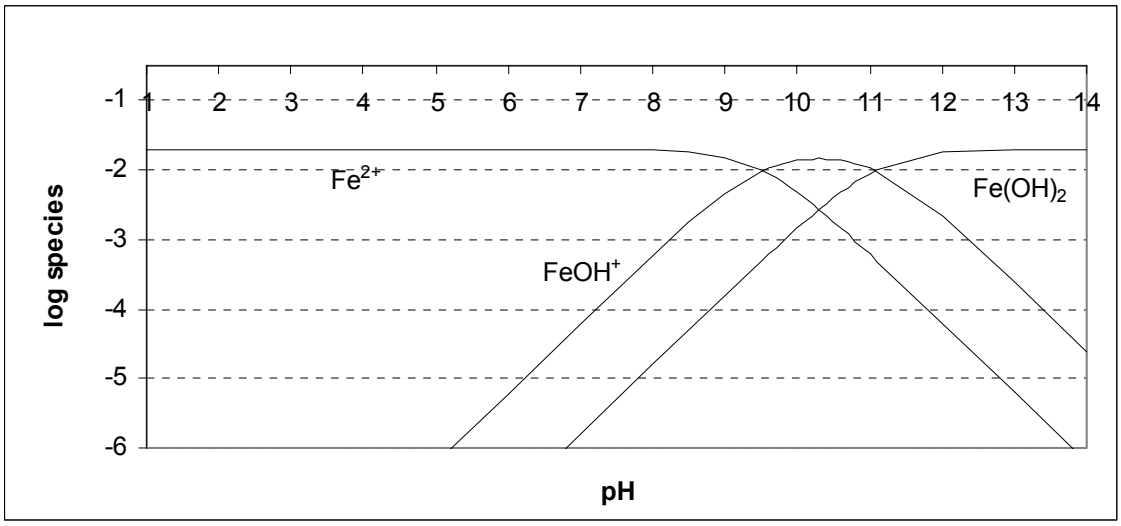

Figure 5.1 Aqueous phase equilibrium for ferrous hydroxide at infinite dilution

In practice, the diagram has little meaning in the higher pH values (above ≈8.5) as $Fe(OH)_{2(s)}$ will precipitate and thus it is never possible to have dissolved Fe^{2+} species ions at the level shown. A more realistic approach is to visualize the system from an aqueous – solid phase equilibrium standpoint.

Aqueous – solid phase equilibrium
The maximum concentration of free metal ions is established via the metal's solubility product equation, i.e. in the case of metal hydroxides

$$[M^{2+}]\,[OH^-]^2 = Ksp' \qquad (5.9)$$

Where Ksp' = apparent solubility product including Debye Huckel effects.

However, the concentration $[M^{2+}]$ in the above equation does not give the total dissolved metal ion species concentration in solution. This arises because M^{2+} forms complexes (dissolved species) as shown in the previous section and the relative concentration of these depends on pH. The total dissolved metal species in solution will be given by the sum of the free and metal hydroxide complexes species concentrations.

The concentration of each of the metal hydroxide complexes at aqueous solid phase equilibrium (Equations 5.4 to 5.6) are determined by linking each of the complex formation equations to the solubility product equation (Equation 5.9). For example, for the concentration of the complex MOH^+ at saturation, solving for $[M^{2+}]$ from Equation 5.4 and substituting into Equation 5.9 gives

$$[MOH^+]\,[OH^-]\,K_{b1}' = K_{sp}' \qquad (5.10)$$

$$\text{i.e. } [MOH^+] = K_{sp}' / ([OH^-]\,K_{b1}') \qquad (5.11)$$

and similarly for the other complexes

$$[M(OH)_2^0] = K_{sp}' / K_{b2}' \quad (5.12)$$

$$[M(OH)_3^-] = K_{sp}' [OH^-] / K_{b3}' \quad (5.13)$$

and so on for higher order hydroxy complexes. The total dissolved metal species in saturation is thus

$$M_T = [M^{2+}] + [MOH^+] + [M(OH)_2^0] + [M(OH)_3^-] \quad (5.14)$$

Such total concentrations of dissolved metal is represented most clearly by taking the logarithms of Equations 5.9, 5.11, 5.12 and 5.13, transforming log $[OH^-]$ to pH and plotting a log species versus pH diagram i.e.

$$\log [M^{2+}] = \log (Ksp') - 2\log(Kw') - 2pH \quad (5.15)$$

$$\log [M(OH)^-] = \log (Ksp') - \log(K_{b1}') - \log(K_w') - pH \quad (5.16)$$

$$\log [M(OH)_2] = \log (Ksp') - \log(Kb_2') \quad (5.17)$$

$$\log [M(OH)_3] = \log (Ksp') - \log(K_{b3}') + \log (Kw') + pH \quad (5.18)$$

In Figures 5.2 to 5.4 are shown plots of log metal species solubility versus pH for the ferrous, nickel and manganese species in water. The various log K_b values are those listed in Table 5.1 and solubility products values are listed below in Table 5.2.

Referring to Figures 5.2 to 5.4, the total dissolved species concentration at any pH is closely equal to the principal species and 0.301 log units above an intercept point. Furthermore, for ferrous, nickel and manganese hydroxide species, the minimum dissolved total metal species concentration is approximately 10^{-7} M at pH 11 for ferrous, 10^{-8} M at pH 10.5 for nickel and 10^{-7} M at pH 12 for the manganese system.

Table 5.2 Solubility product constants for various metal hydroxides

Precipitant	***Log Ksp***	***Reference***
$Fe(OH)_2$	*-15,1*	*Stumm and Morgan (1996)*
$Mn(OH)_2$	*-12,8*	
$Zn(OH)_2$	*-16,0*	
$Ni(OH)_2$	*-14,7*	

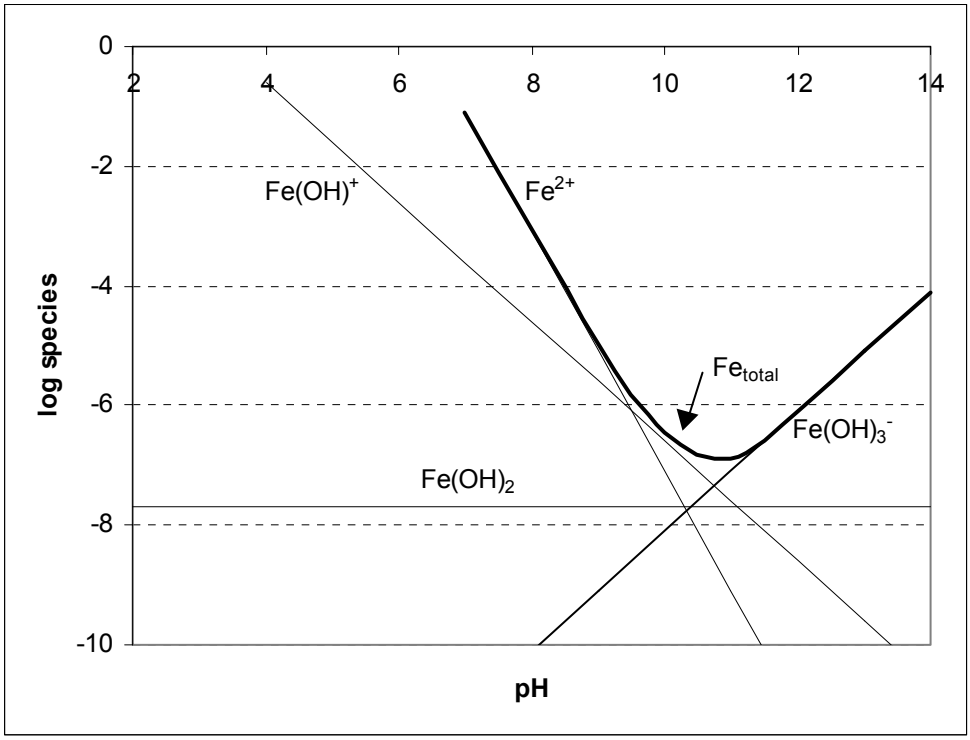

Figure 5.2 Aqueous and solid phase equilibrium for ferrous hydroxide at infinite dilution

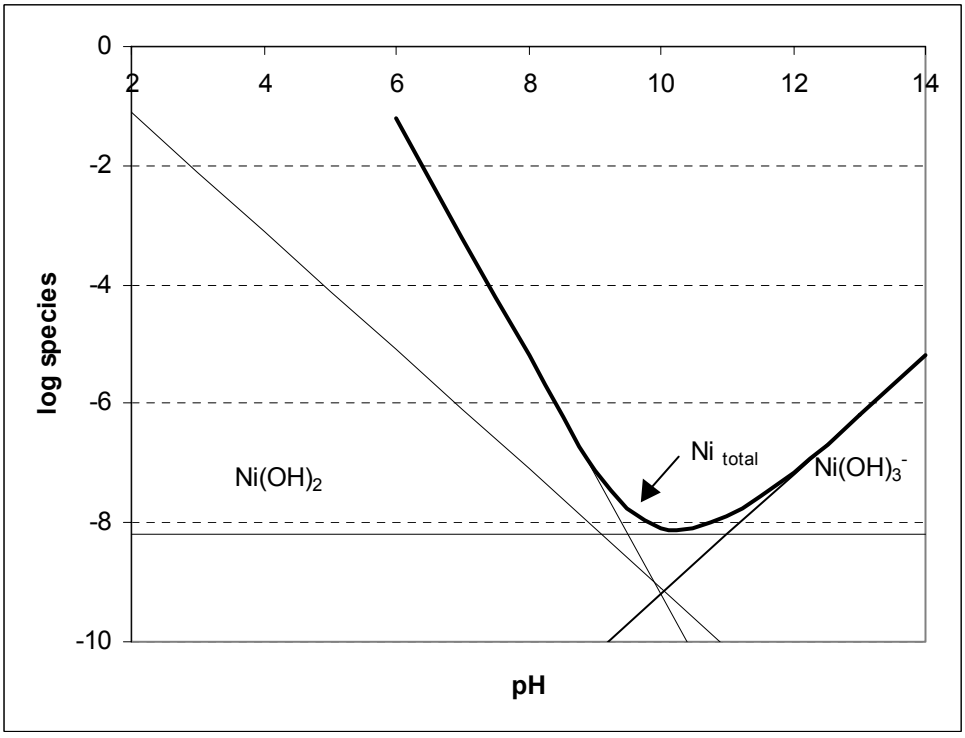

Figure 5.3 Aqueous and solid phase equilibrium for nickel hydroxide at infinite dilution

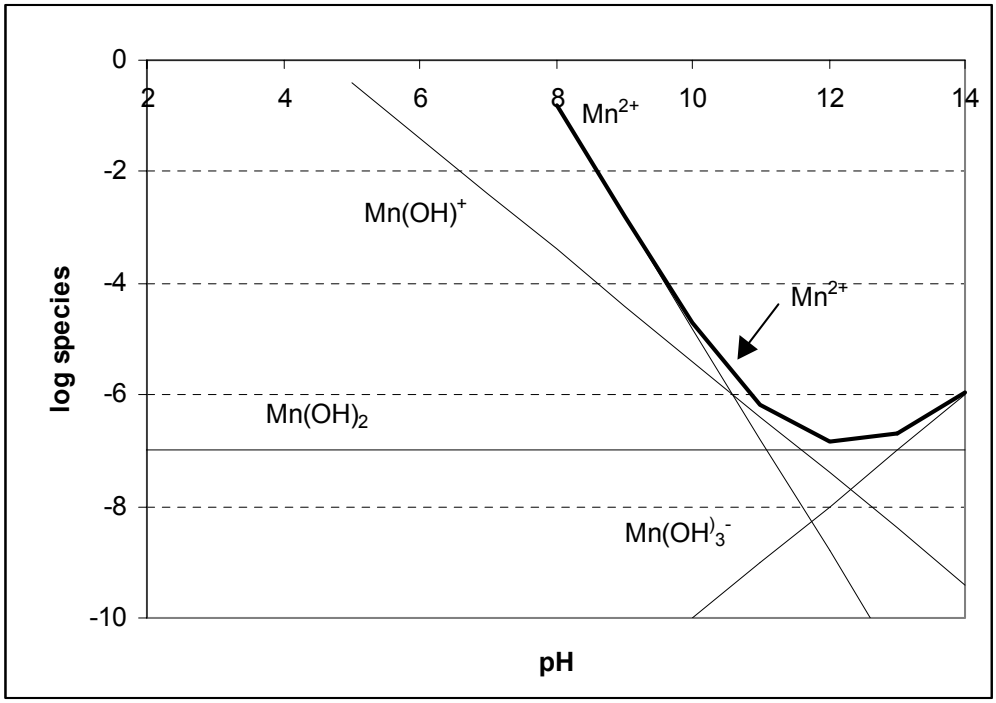

Figure 5.4 Aqueous and solid phase equilibrium for manganese hydroxide at infinite dilution

5.3 HEAVY METALS – SULPHIDE SYSTEM

Aqueous phase

The sulphide system comprises a diprotic weak acid system in aqueous solution, H_2S, HS^- and S^{2-}. However, reported data on the dissociation between HS^- and S^{2-} is so variable ($12 < pK_a < 19$) that direct use of the species S^{2-} in not feasible. Consequently, only weak acid equilibrium between HS^- and H_2S species are normally considered, and solubility products are measured and reported relative to the HS^- species. Considering equilibrium in the aqueous phase

$H_2S \Leftrightarrow H^+ + HS^-$ *giving*

$$[H^+]\,[HS^-] / [H_2S] = K_a \qquad (5.19)$$

Where pKa ≈ 7.1 at 20 °C.

The mass balance equation for the sulphide species neglecting $S^{2-}$is

$$S_T = [H_2S] + [HS^-]_T \qquad (5.20)$$

Where S_T = total dissolved sulphide species concentration and $[HS^-]_T$ = free and metal complexed HS^- species.

Examining the above two equations shows that the species of interest HS^- and H_2S vary with both pH and S_T. This makes solubility computation more difficult than for the hydroxide species discussed previously where the precipitating ligand OH^- varies directly with pH.

For most of the metal species of significant concentration in AMD waters, metals sulphide complexing is not reported, an exception being cadmium. These two scenarios (with and without complexing) require different treatment in determining dissolved metal ion concentration expected and are consequently dealt with separately.

Aqueous – solid phase equilibrium (no metal sulphide complexing)

Current convention is to report metal sulphide solubility products in terms of HS^- because of the uncertainty associated with the HS^-/S^{2-} dissociation constant, i.e. in terms of the reaction $MS + H^+ \Leftrightarrow M^{2+} + HS^-$ with the corresponding solubility product equation

$$[M^{2+}]\,[HS^-] / [H^+] = K_{sp}' \qquad (5.21)$$

Note that when solubility product data is to be used relative to S^{2-} , the user should always ensure that the HS^-/S^{2-} dissociation constant used comes from the same source as the corresponding K_{sp} value.

The precipitating ligand, HS^-, depends on S_T and pH as follows (derived from Equations 5.20 and 5.21)

$$[HS^-] = S_T K_a' / \{K_a' + [H^+]\} \qquad (5.22)$$

Substituting this equation into the solubility product expression and simplifying gives the dependence of M^{2+} on pH and S_T at two-phase equilibrium

$$[M^{2+}] = K_{sp}'\,[H^+]\,\{K_a' + [H^+]\} / (S_T\,K_a') \qquad (5.23)$$

Taking logarithms yields

$$\log [M^{2+}] = pK_a' - \log S_T - pK_{sp}' - pH + \log \{ K_a' + [H^+]\} \qquad (5.24)$$

Graphical presentation is now easily effected as follows

In the region $pH<pK_a$ (i.e. $[H^+]>>K_a'$)

$$\log [M^{2+}] = pK_a' - \log S_T - pK_{sp}' - 2\,pH \qquad (5.25)$$

In the region where $pH = pK_a'$ (i.e. $[H^+] = K_a'$)

$$\log [M^{2+}] = -\log S_T - pK_{sp} - pH + \log 2 \qquad (5.26)$$

and where $pH>pK_a'$ (i.e. $[H^+]<<K_a'$)

$$\log [M^{2+}] = -\log S_T - pK_{sp} - pH \qquad (5.27)$$

In Figure 5.5 is shown plotted log $[Fe^{2+}]$ solubility with pH for FeS precipitation and values of S_T of 10^{-6}, 10^{-5} and 10^{-4} M. Using pK values listed in Table 5.3.

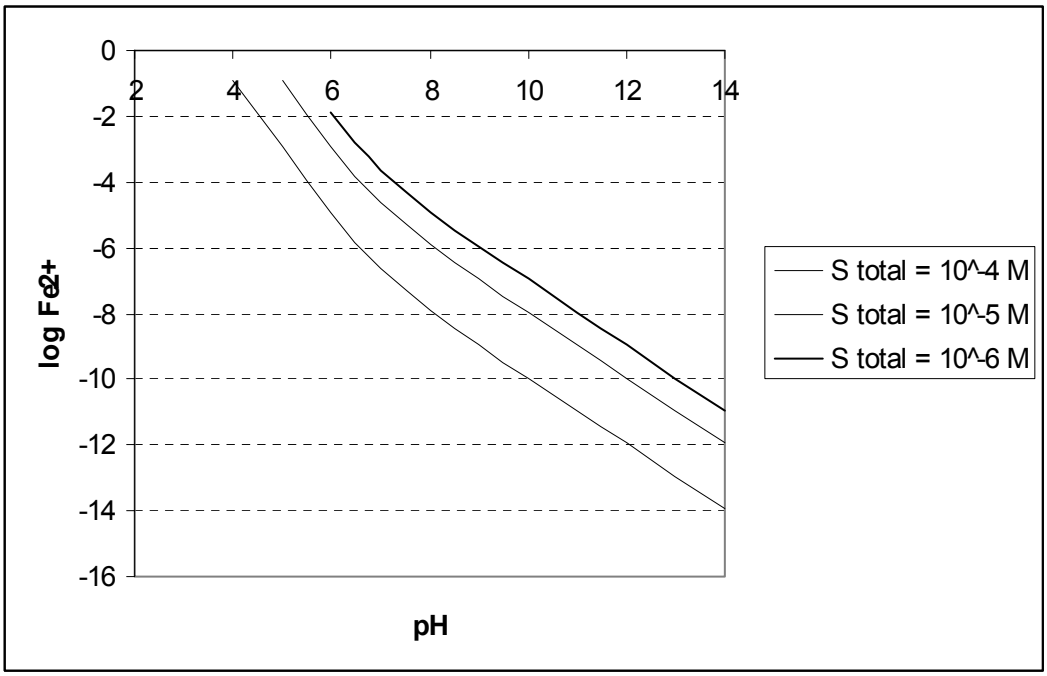

Figure 5.5 Plots of residual iron in solution vs. pH for various S_T values

A comparison of various metal ion solubilities can be effected using the above approach. From Figure 5.5 it is apparent that at relatively low pH values, for example pH 6 and S_T of 10^{-4} M, the total dissolved Fe^{2+} concentration is as low as 10^{-5} M. In comparison, for $Fe(OH)_2$ governing solubility, at pH 6 the solution would have an extraordinarily high Fe_T value (see Figure 5.2).

Table 5.3 Dissociation constants for H_2S and metal solubility products for the reactions

$H_2S \Leftrightarrow H^+ + HS^-$ and $MS + H^+ \Leftrightarrow M^{2+} + HS^-$

Precipitant	**log K_s** (source: Dyrssen and Kremling, 1990)
FeS (amorphous)	-2.95
NiS	-5.6
MnS	-3.34

In Figure 5.6 is shown metal ion in solution with pH for the metal species Fe^{2+}, Ni^{2+} and Mn^{2+} and a total sulphide in solution of 10^{-5} M.

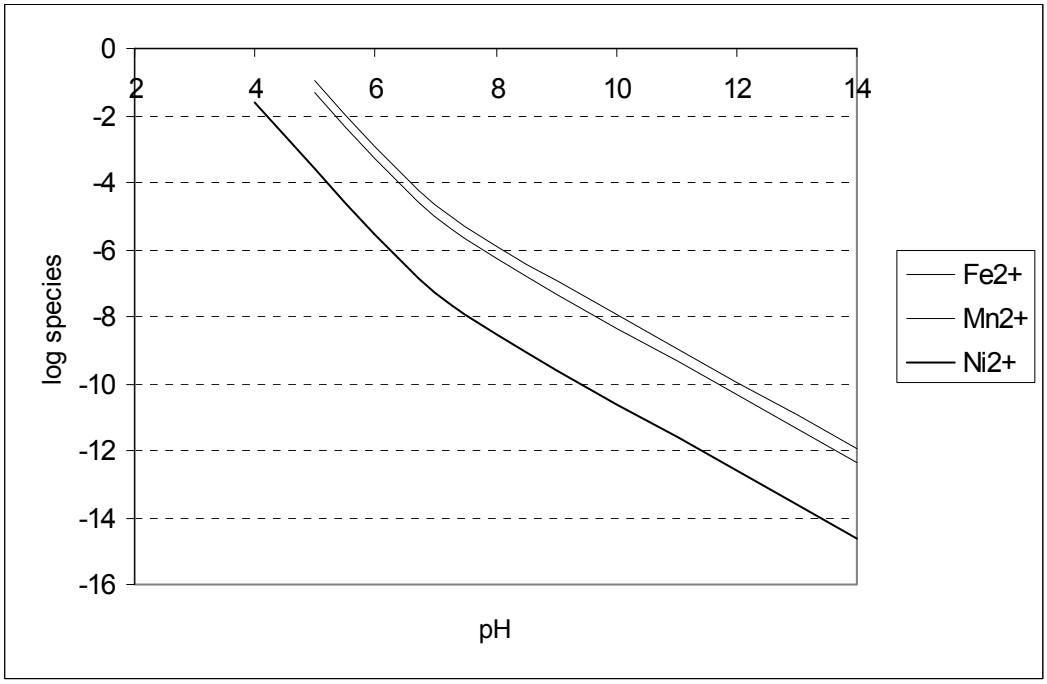

Figure 5.6 Solubility of various metal ion species with pH for $S_T = 10^{-5}$ M

Equations 5.25 to 5.27 can easily be used to obtain further insight into the metal sulphide solubilities, for example keeping pH constant and plotting log $[M^{2+}]$ versus S_T as shown in Figure 5.7.

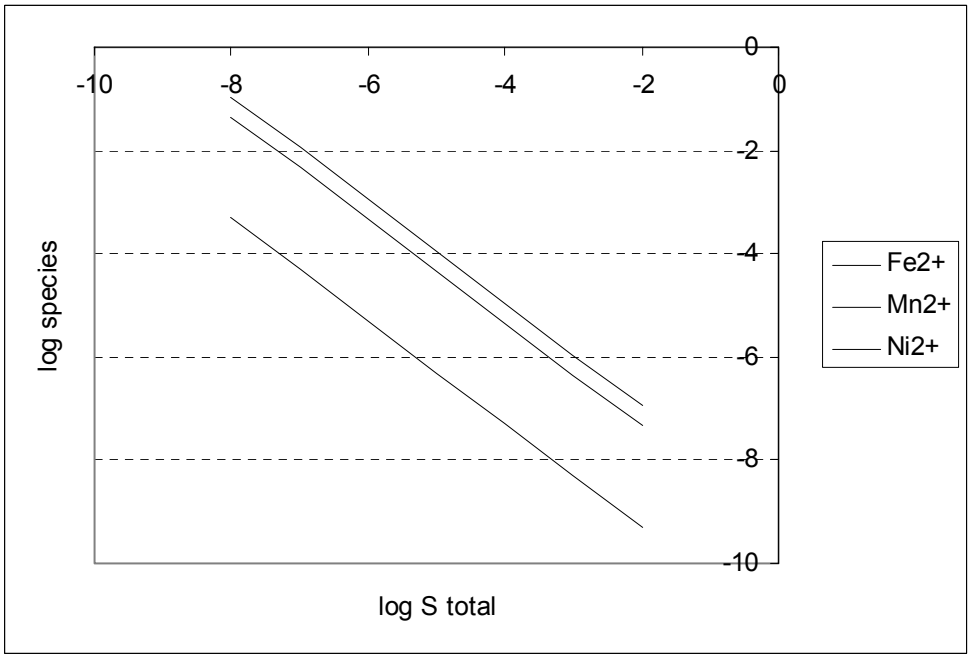

Figure 5.7 Solubility of various metal ion species at pH 6 for various concentrations

Aqueous-solid equilibrium with metal ion complexing

For aqueous – solid phase equilibrium of metal sulphides where sulphide complexing is reported (together with the solubility product) the approach is to formulate equations for the solid mineral in terms of each of the metal sulphide complexes, $[H^+]$ and S_T. This is achieved

by combining the solubility product and complex formation equations. For example, if a metal sulphide complex MHS^+ is reported, the equilibrium dissociation equation is

$$[M^{2+}]\,[HS^-] / [MHS^+] = K_{c1}{}'^{6} \qquad (5.28)$$

and the solubility product equation is

$$[M^{2+}]\,[HS^-] / [H^+] = K_{sp}{}' \qquad (5.29)$$

The equation and equilibrium constant for the complex in the cadmium form is $MS_{(s)} + H^+ \Leftrightarrow CdHS^+$ with some K_x value. Rearranging (5.28) and (5.29) above gives the appropriate equilibrium equation

$$[MHS^+] / [H^+] = K_s{}' / K_{c1}{}' = K_x{}' \qquad (5.30)$$

As an example, consider the metal Cd^{2+} for which the sulphide complexes $Cd(HS)^+$, $Cd(HS)_2{}^0$, and $Cd(OH)S^-$ are reported in conjunction with a solubility product for $CdS_{(s)}$ (Daskalakis and Heltz, 1992). The appropriate forms for depicting the system (and the corresponding adjusted equilibrium constants) are

$CdS_{(s)} + H^+ \Leftrightarrow Cd^{2+} + HS^-$	(pK_{sp} = +14,35)
$CdS_{(s)} + H^+ \Leftrightarrow Cd(HS)^+$	(pK_1 = +6,7)
$CdS_{(s)} + H^+ + HS^- \Leftrightarrow Cd(HS)_2{}^0$	(pK_2 = +1,0)
$CdS_{(s)} + H_2O \Leftrightarrow Cd(OH)S^- + H^+$	(pK_3 = +16,8)

Taking logarithms of the equilibrium equations for the above reactions and solving for the logarithm of each of the complex species concentrations at aqueous phase equilibrium gives

$$\log [Cd(HS)^+] = -pK_1 - pH \qquad (5.31)$$

$$\log [Cd(HS)_2{}^0] = -pK_2 - pH + \log [HS^-] \qquad (5.32)$$

$$\log [Cd(OH)S^-] = -pK_3 + pH \qquad (5.33)$$

Referring to equation (4.32) above, the species concentration $[HS^-]$ varies with pH and S_T (as explained earlier) i.e. $[HS^-] = S_T\,K_a' / (K_a' + [H^+]) \approx S_T\,K_a{}' / [H^+]$ at $pH < pK_a{}'$.

Consequently, at $pH < pKa{}'$, equation (32) becomes

$$\log [Cd(HS)_2{}^0] = -pK_2{}' + \log S_T - pK_a{}' \qquad (5.34)$$

and similarly for log [Cd2+] where $pH<pK_a{}'$

$$\log [Cd^{2+}] = -pK_s{}' - \log S_T + pK_a{}' \qquad (5.35)$$

Equations (5.31), (5.33) and (5.35) allow a very simple graphical depiction of aqueous-solid phase equilibrium situation at a particular pH as shown in Figure 5.8 or alternatively with a total dissolved sulphide species concentration.

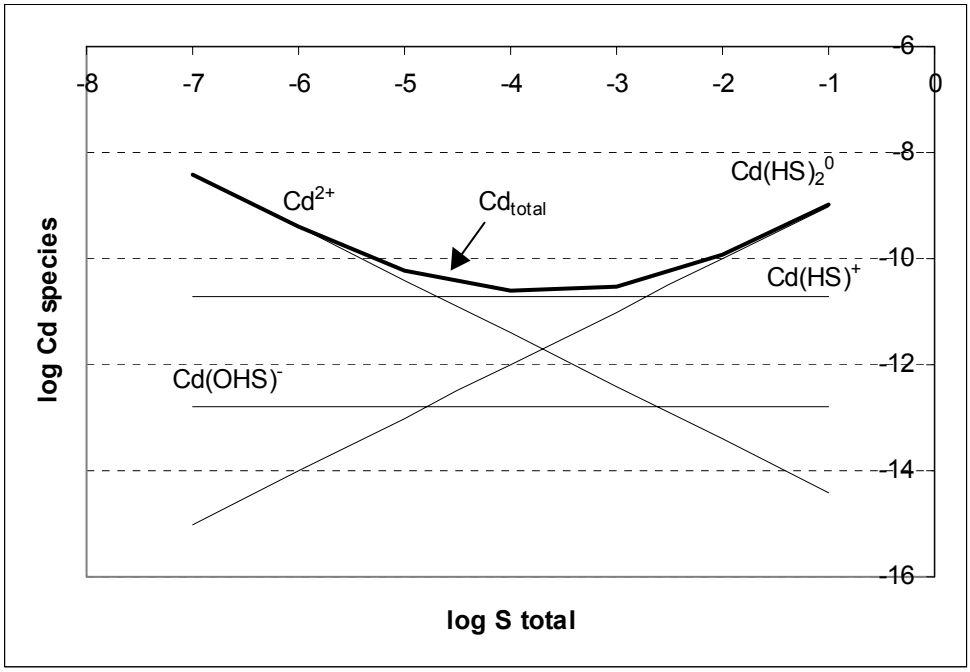

Figure 5.8 Aqueous – solid phase equilibrium for cadmium sulphide species at pH 4 and variable dissolved sulphide concentrations

5.4 PRACTICAL CONSIDERATIONS FOR IRON AND HEAVY METALS REMOVAL FROM AMD WATERS IN THE GAUTENG AREA

Most of the AMD waters in the Gauteng region contain *inter alia* Fe^{2+} concentration of above 1200 mg/l, Mn^{2+}>30 mg/l, Ni^{2+}>15 mg/l, Al^{3+}>60 mg/l accompanied with high SO_4^{2-} concentrations (>4000 mg/l). For these waters neither of the precipitants $M(OH)_2$ nor MS is useful *per se* in a treatment process. The metal hydroxides are too voluminous with poor liquid-solids separation properties. Furthermore, the metals are easily leached from the solid phase during disposal and at the disposal site at a relatively high pH value. To effect permanent fixing of the metals, further costly sludge treatment need to be effected.

On the other hand, problems also arise with a metal sulphide removal process because the principal metal sulphide species FeS forms a colloidal precipitant, with poor settling properties. However, the current treatment process (the HDS process) involves firstly oxidation of the iron and thereafter removal of a conditioned good-settling precipitant. Minimal removal of heavy metals occurs in this process. Consequently, there may yet be a role for metal sulphides removal as a secondary treatment unit process. This would involve removal of the remaining heavy metals using sulphide with addition (or *insitu* generation of Fe^{3+}) of a coagulant to attain efficient liquid – solid separation. However, such a system will probably be inhibited by cost considerations.

In light of the above, a metal oxide precipitation (FeOOH and Fe_3O_4/ferrite) process can be considered as a means of complete removal of iron and heavy metals in a single process, without the necessity for further sludge treatment.

5.5 METAL OXIDES (THE FERRITE PROCESS) – AN ALTERNATIVE APPROACH TO IRON AND HEAVY METALS REMOVAL FROM AMD AT AMBIENT TEMPERATURE

The conventional approach to iron removal from AMD consists of the so-called High Density Sludge process (HDS). In this process ferrous ions are oxidized to ferric at high oxygen concentration and relatively low pH. The ferric subsequently precipitates and settles (at pH 6) as amorphous ferric hydroxide (ferrihydrite) which upon dehydration changes to FeOOH and Fe_2O_3 as the final products. In order to induce crystallization and settling properties, the sludge is recycled and brought in contact with the lime in a conditioning tank before the AMD water is introduced. This process, although proven efficient for iron removal, has no capability of removing heavy metals.

The Ferrite Process constitutes an alternative approach to iron and heavy metals removal from AMD waters. The term 'ferrite' refers to magnetic oxides containing other metals in addition to iron. The general chemical formula of ferrites is MFe_2O_4, where M is any divalent ion with an unhydrated ion radius between app. 0.6 and 1 A. A well known example is iron ferrite or magnetite, where iron is the only metallic constitute (Wang et al., 1996).

Theoretical pathways for ferrite formation

Ferrite is formed via partial oxidation of ferrous species at pH values greater than 7.The ferrite formation reaction has been shown to proceed through two pathways depending on pH and rates of oxidation. At pH values ranging from 7 to 10 and relatively slow oxidation rates, ferrites form through the Green Rust (GR) path whilst at a pH of 10.5 and above, the ferrites form not through GR but from the γ- FeOOH phase (Tamaura et al., 1991). Green rusts are defined as unstable green-blue compounds consisting of a mixture of ferric and ferrous ions accompanied by Cl^-, SO_4^{2-} or CO_3^{2-} and hydroxide anions firstly described by Keller in 1948 (Cuttler et al., 1990). Green rusts belong structurally to the sjogrenite-pyroaurite class of hydroxides, consisting of alternating positively charged trioctahedral metal hydroxide layers ($Fe^{2+}(OH)_6$, in which some of the ferrous is replaced by ferric) balanced by negatively charged interlayers of anions located between the layers (Schwertmann and Fechter, 1993; Hansen et al., 1994). Green rusts are classified via the group of anions located between the octahedral iron layers as GR1 (chlorides), GR2 (sulphate) and carbonated GR.

Because of the preference for divalent over monovalent anions in the interlayer (Miyata, 1983), GR2 and carbonated GR will prevail over GR 1 in acid mine drainage. Moreover, because SO_4^{2-} concentration is much higher than the carbonate system concentration in such waters, GR2 will probably be the dominant species. Green Rust 2 has been reported to form in at least two different path ways. The first is

Aerial oxidation of Fe^{2+} ions, $Fe(OH)^+$ or $Fe(OH)_2$ to a hydrous, poorly ordered ferric hydroxide (ferrihydrite containing 0.65 mole of anions (not hydroxides) per mole of ferric) at pH around 7. Ferrihydrite in turn reacts with dissolved Fe^{2+} ions at neutral pH values to form GR through the following reaction (Fox, 1988; Hansen, 1994)

$$2Fe(OH)_{2.35}(SO_4)_{0.325(s)} + 4Fe^{2+}{}_{(aq)} + 7.3(OH)_{(aq)} + 0.675SO_4{}^{2-}{}_{(aq)} + 3H_2O_{(l)} \Leftrightarrow [Fe_4^{II}Fe_2^{III}(OH)_{12}][SO_4 \cdot 3H_2O] \quad (5.36)$$

And the second is

Direct precipitation of GR from an initial mixture of ferric and ferrous ions at neutral/slightly basic pH values through the same reaction (Hansen, 1994).

Several authors, including the writers have observed that ferrite formation through the GR2 pathway (pH<10) results in relatively high residual iron and heavy metals concentrations, and inferior sludge settling properties (Perez et al., 1998; Kiyama, 1974). Conversely, ferrite formation at pH>10 results in excellent efficiency removal (>99.9%) and improved sludge settling properties.

Barrado et al. (1998) proposed the following reactions for ferrite formation from ferrous at pH > 10.5

In the absence of heavy metals and controlled oxidation rate

$$3FeSO4 + 6NaOH + 0.5O_2 \rightarrow Fe_3O_4 + 3Na_2SO_4 + 3H_2O \quad (5.37)$$

In the presence of heavy metals and controlled oxidation rate

$$xMe^{+n} + 3FeSO_4 + 6NaOH + 0.5O_2 \rightarrow Me_xFe_{3-x}O4 + 3Na_2SO_4 + 3H_2O + xFe^{+n} \quad (5.38)$$

Fe^{+n} represents the total concentration of iron whose precipitation as ferrite is impeded by the other metal cations present in the water. The displaced iron can appear as ferrous or ferric depending on the valency of the displacing cation. If the pH of the solution is maintained above 10 these ferrous and ferric ions will react again to form magnetite.

In excess of oxidizing agent goethite is formed instead of magnetite

$$2Fe^{2+} + 0.5O_2 + 4OH^- \rightarrow 2\ \alpha\text{-}FeOOH + H_2O \quad (5.39)$$

Current research and applications of the 'ambient temperature ferrite process'

The ferrite process was principally aimed at heavy metal removal from laboratory wastewater in Japan. The heavy metals are incorporated into the lattice points of the ferrite. In a typical process, $FeSO_4$ is added to the solution to bring the iron/heavy metals molar ratio to between 10 and 20, the pH is raised to 9-11, the temperature to 65^oC and oxygen is added to partially oxidize ferrous to ferric. The precipitates of the ferrite process are stable and readily recovered by magnetic filtration (Tamaura et al., 1991). Furthermore, the heavy metals are not leached from the sludge on aging, as they are incorporated into the lattice. An additional incentive to pursue the ferrite process is the potential commercial use of ferrite as recording media, magnetic markers and steel making feeds (Wang et al., 1996). However, the high temperature applied in the standard ferrite process would appear to reduce practical implementation.

The ferrite process has been also investigated in the context of heavy metals removal from AMD at ambient temperature. Tamaura et al. (1991) reports on an attempt made in Japan to oxidize a part of an AMD stream to ferrihydrate (amorphous ferric hydroxide), which is subsequently applied to the Fe^{2+} containing main stream ions to form ferrites. Yang et al. (1995, cited in Wang et al., 1996) suggested a ferrite process in which only the sludge is heated, the drawback reported was poor settling and therefore poor solid/liquid separation. Wang et al. (1996) reported on a modified ambient-temperature ferrite process for the removal of iron and heavy metals from AMD in Canada. They asserted that in the presence of ferric there is no need to heat the water to obtain ferrite (in the absence of ferric the phase diagram of iron-water-temperature system indicates formation of pure Fe_3O_4 only at

temperatures higher that 60^{o}C, whilst at ambient temperatures various quantities of FeO(OH) + magnetite are formed). The authors concentrated on the best initial conditions to attain the best magnetic properties of the end product. Their results show that a Fe^{3+} to Fe^{2+} ratio of 2 to 1 and a pH of above 9.5 gives the best ferrite recovery (around 96%) and the best magnetic properties. Zinc, aluminium and magnesium as well as calcium were removed as a part of the crystal structure of the ferrite. The presence of calcium had an adverse effect on the ferrite process, reducing metal recovery, magnetization and ferrite stability (Wang et al., 1996).

Perez et al. (1998) also concluded that a precipitation pH between 10 and 11 and a moderate air injection are suitable conditions for quick generation of magnetite at ambient temperatures.

REFERENCES TO CHAPTER 5

BARRADO, E, PRIETO, F, VEGA, M, and FERNANDEZ-POLANCO F (1998) Optimization of the operational variables of a medium-scale reactor for metal-containing wastewater purification by ferrite process. Water Res. **32**(10), 3055-3061.

CUTTLER, A H, CRANSHAW, T E, and LONGWORTH, G (1990) A Mossbauer study of green rust precipitates: 1. Preparations from sulphate solutions. Clay Minerals, **25**, 289-301.

DASKALAKIS K D and HELZ, G R (1992) Environ. Sci. Technol. **26**, 2462.

DRYSSEN, D and KREMLING, K (1990) Increasing hydrogen sulphide concentration and trace metal behavior in the anoxic baltic waters. Mar. Chem. **30**, 193-204.

FOX, L E (1988) The solubility of colloidal ferric hydroxide and its relevance to iron concentrations in river water. Geochim. Cosmochim. Acta **52**, 771-777.

HANSEN, H C B, BORGGAARD, O K and SORENSEN, J (1994) Evaluation of the free energy of formation of Fe(II) - Fe(III) hydroxy-sulphate (green rust) and it's reduction to nitrite. Geochinica et Cosmochimica Acta **58**(12), 2599-2608.

KIYAMA, M (1974) Conditions for the formation of Fe_3O_4 by the air oxydation of $Fe(OH)_2$ suspensions.

MIYATA, S (1983) Anion-exchange properties of hydrotalcite-like compounds Clays Clay Minerals **31**, 305-311.

PEREZ, O P, UMETSU, Y and SASAKI, H (1998) Precipitation and densification of magnetic iron compounds from aqueous solutions at room temperature. Hydrometallurgy, **50**, 223-242.

SCHWERTMANN, U and FECHTER, H (1994) The formation of green rust and its transformation to lepidocrocite. Clay Minerals, **29**, 87-92.

STUMM, W and MORGAN, J J (1996) Aquatic chemistry. John Wiley & Sons, INC.

TAMAURA, Y, KATSURA, T, ROJARAYANONT, S, YOSIDA, T, and ABE, H (1991) Ferrite process; heavy metal ions treatment system. Water Sci. Tech., 1893-1900.

.

WANG, W, ZHENGHE, X U and FINCH, J (1996) Fundamental study of an ambient temperature ferrite process in the treatment of acid mine drainage. Environ. Sci. Technol. **30**, 2604-2608.

CHAPTER 6

CONCLUDING REMARKS

The research presented in this report must be considered as a preliminary study into feasibility of applying biological – physical – chemical treatment processes to AMD waters. It forms a parallel study to that being effected at Rhodes University, in which an overall low cost treatment process for the removal of pollution arising from mining activities is being investigated.

Over and above, a fundamental thermodynamic equilibrium investigation into metal and S species in the AMD environment was carried out. Preliminary experimental studies were effected on possible practical solution procedures to both S species and metal ion removal. With regard to the S removal, only removal of species in the reduced state (i.e. H_2S, HS^-, S^{2-}) were considered – these in fact are the species generated within the Rhodes process.

Consideration of future work in metal ion removal
With regard to sulphide species removal: 2 alternatives to the Rhodes process were considered. The first is using membranes permeable only to sulphide (i.e. silicone membranes). In this investigation the sulphide-rich liquid was pumped through silicone tubes of varying thickness. The tubes were immersed in a ferric solution in which H_2S species were partially oxidised to elemental sulphur. At pH values lower than 6, sulphides appear almost exclusively in the liquid phase as H_2S, which penetrated the silicone tube and was collected in the ferric solution where it was oxidised to elemental sulphur. Kinetic measurements on the process showed the proposal to be impractical from an engineering standpoint (the rate limiting kinetics was the permeability of the silicone membrane).

Second, the dissolved sulphide species in the effluent were stripped using CO_2 as a carrier gas. The carrier gas was them bubbled through acidified ferric solution generating elemental sulphur. The carrying CO_2 gas was then recycled. Kinetics of this process would indicate that this process is practical from an engineering standpoint, and warrants further investigation.

Acid mine drainage (AMD), impacts negatively on freshwater resources in the mining areas of South Africa, and many other parts of the world. AMD waters are characterised by low pH, very high iron concentrations, significantly high concentrations of non-ferrous (mainly heavy) metals, and very high salinity, principally in the form of sulphate. The chemical makeup of AMD is directly explicable in terms of the biogeochemical process whereby AMD arises: put most simply, mining activities allow atmospheric oxygen and water to contact and, together with the action of aerobic bacteria, oxidise iron pyrite (FeS_2) in the rock. This releases sulphate and iron into underground water making the latter strongly acidic, causing leaching of non-ferrous metals from the rock (Kleinmann et al., 1981). A comprehensive solution to AMD pollution requires both metal and sulphate removal. The latter can be effected by either biological or membrane-based methods.

In the treatment of AMD iron and non-ferrous metals may be precipitated as hydroxides ($M(OH)_2$), sulphides (MS), oxides (MO_x), and rarely as carbonates. The species that precipitate in any scenario will depend on the nature and concentrations of precipitation ions and *inter alia* on pH, temperature, redox potential and rates of chemical addition (i.e. mixing configuration).

Most of the AMD waters in the Gauteng region in South Africa contain Fe^{2+} concentration of above 1200 mg/l, Mn^{2+}>30 mg/l, Ni^{2+}>15 mg/l, Al^{3+}>60 mg/l accompanied with high SO_4^{2-} concentrations (>4000 mg/l). For these waters neither of the precipitants $M(OH)_2$ nor MS are useful *per se* in a treatment process. Metal hydroxides are too voluminous and have poor liquid-solid separation properties. Furthermore, such sludge is unstable easily leached from the solid phase during disposal and at the disposal site at a relatively high pH value. To effect permanent fixing of the metals, further costly sludge treatment needs to be effected.

On the other hand, problems also arise with a metal sulphide removal process because the principal metal sulphide species FeS forms a colloidal precipitant, with poor settling properties. Furthermore, each metal sulphide precipitates optimally at different conditions. Consequently, in the South African context such a system will probably be inhibited by cost considerations. In light of the above, a metal oxide precipitation process should be considered as a means of complete removal of iron and heavy metals in a single process, without the necessity for further sludge treatment.

Current strategies for metal removal from AMD have several shortcomings (Loewenthal et al., 2001; Bosman, 1983). The High Density Sludge (HDS) process, deployed on several South African mines, utilises lime for pH adjustment and oxygen to vigorously oxidise ferrous iron. A recycle loop is used to densify the ferrihydrite precipitant which is otherwise difficult to separate from the liquid phase. Minimal non-ferrous metals are removed and high oxygen concentrations are required. These limitations, coupled with the magnitude of the AMD problem (some mining basins pump up to 60 000 m^3 of water per day), underscore the need for improved cost-effective treatment methods.

Magnetite is a partially oxidised iron oxide with the formula Fe_3O_4 (i.e. $Fe^{3+}{}_2Fe^{2+}O_4$). It thus conforms to the general formula $M1^{3+}{}_2M2^{2+}O_4$ for ferrites, where M1 and M2 stand for any of a number of possible metal elements. Magnetite is therefore a ferrite in which the metal component is made up purely of iron. If a solution dominated by soluble iron but containing smaller concentrations of other divalent and trivalent metal species (such as are found in AMD) is transformed into ferrite, then the resulting precipitant will be dominated by magnetite but some of the iron atoms will be replaced by non-ferrous cations, making for "substituted magnetite" or "mixed-species" ferrites.

Barrado et al. (1998) proposed the following stoichiometric reactions for ferrite formation from ferrous at pH > 10.5

In the absence of heavy metals and with a slow oxidation rate

$$3Fe(OH)_2 + 3SO_4^{2-} + 6Na^+ + 0.5O_2 \rightarrow Fe_3O_4 + 3Na_2SO_4 + 3H_2O \quad (6.1)$$

Equation 1 shows that alkalinity is neither produced nor consumed during the formation of magnetite from ferrous hydroxide with oxygen acting as electron acceptor, and that 0.47 mg/ℓ of magnetite (as Fe) are formed for every 1 mg/ℓ of oxygen consumed.

In the presence of heavy metals and with a slow oxidation rate

$$xMe^{+n} + 3Fe(OH)_2 + 3SO_4^{2-} + 6Na^+ + 0.5O_2 \rightarrow Me_xFe_{3-x}O_4 + 3Na_2SO_4 + 3H_2O + xFe^{+n} \quad (6.2)$$

Fe^{+n} represents the total concentration of iron which is replaced by metal cations in the ferrite structure. This displaced iron will appear as ferrous or ferric depending on the valence of the displacing cation. These ferrous and ferric ions will react to form magnetite.

However it is to be noted that with excess oxidising agent goethite is formed instead of magnetite

$$2Fe^{2+} + 0.5O_2 + 4OH^- \rightarrow 2\ \alpha\text{-}FeOOH + H_2O \qquad (6.3)$$

The formation of relatively pure precipitates of magnetite from ferrous solutions was until recently only thought to be possible at temperatures greater than 90 degrees centigrade (Kiyama, 1974; Cornell and Schwertmann, 1996). Nevertheless, the capacity of magnetite to absorb by substitution non-ferrous metals, plus the advantageous settling properties of magnetite, have resulted in the exploitation of magnetite formation as a means to remove metal ions from waste streams. The "ferrite process" refers to a high temperature process (65 degrees C) developed in Japan for the treatment of laboratory wastes containing heavy metals (Katsura et al., 1977; Tamaura et al., 1991a and 1991b). However during the last decade, several developments in the field of ambient temperature ferrite chemistry have occurred which appear to be opening the way to treating large volumes of water such as AMD.

Tamaura et al. (1991b) first applied the ferrite process at ambient temperature as a *two-step* process in which a ferrous AMD stream is split into two. One stream is oxidised to ferric and the streams are then recombined at an elevated pH whereupon magnetite is formed. Wang et al. (1996) found the optimum ferric : ferrous ratio for ambient temperature magnetite formation to resemble the stoichiometric ratio (i.e. 2 : 1) of these ions in magnetite. These authors also investigated the effects of both non-ferrous metals (as found in a Canadian AMD) and calcium on ambient temperature ferrite formation. Finding that calcium, but not non-ferrous metals, interfered decisively with ferrite formation, this same group investigated the effects of magnetite seed. It was found that magnetite seed restored the capacity for ferrite formation at ambient temperature in the presence of calcium; and a "seeded ambient temperature ferrite process" for AMD was presented. This scheme requires stoichiometric adjustment by supplementary ferrous salt addition (McKinnon et al., 2000). Earlier, Perez et al. (1998) found that recycling of magnetic precipitates formed *during* the oxidation of ferrous sulphate solutions in the presence of calcium had a positive effect on ferrite formation at ambient temperature.

The potential for mixed-species ferrite formation at ambient temperature in the presence of calcium using seed thus appears possible as either a one-step, in-line oxidation procedure or by a two-step, split-stream stoichiometric combination procedure. At present there is no indication that one of these two methods is superior. Indeed the sparse literature on ambient temperature ferrite formation reflects the infancy of this field and in particular there is little published information with respect to key process parameters such as kinetics, heavy metal substitution, effect of calcium, settling behaviour, and sludge stability. Preliminary studies conducted by the writers confirmed the feasibility of the one-step approach. On the basis of this, plus the cost advantages of a one-step process, a systematic investigation into the fundamentals of a one-step ambient temperature ferrite process for treatment of AMD was initiated.

Reaction pathways followed and intermediate and end-products generated during the oxidation of ferrous solutions vary according to conditions of pH, temperature, concentration of reactants, presence and type of anions, mixing conditions, etc. In ways which are complex and poorly understood (Sugimoto and Matijevic, 1980; Blesa and Matijevic, 1989; Cornell and Schwertmann, 1996). By and large, conditions inducing magnetite formation from ferrous solutions (in the absence of seed) are slow oxidation, strongly alkaline pH, high ferrous concentrations and high temperature (Cornell and Schwertmann, 1996).

Given the well-proven ability of magnetite to absorb non-ferrous metals from solution in the high temperature ferrite process mentioned above, the environmental conditions for ambient temperature magnetite formation were investigated as a first step towards an ambient temperature ferrite process for the treatment of AMD.

Towards this end, magnetite formation was investigated with respect to the following parameters: seed : initial ferrous ratio, airflow rate, pH and temperature.

The results reported in extension to this report illustrate that the use of seed facilitates the formation of magnetite by the aerial oxidation of AMD at ambient temperature. For reasons of simplicity, the investigation is confined initially to magnetite formation using seed at ambient temperature via the oxidation of pure ferrous sulphate solutions, and does not address the issues of non-ferrous metals or calcium, although these are mentioned. The emphasis of this work is to properly understand and quantify the conditions underlying magnetite formation as applied to AMD in order to design and implement a treatment process. The role of these other elements will be also systematically introduced in this future work. Other aspects relevant to a magnetite seed-based process, such as kinetics of oxidation, sludge settlement, sludge impurities and sludge stability are also discussed.

PARTICULAR STUDIES ON THE RHODES PROCESS

With regard to particular studies effected on the Rhodes process it was found:

I. Blending untreated AMD waters with sulphide recycled waters results in floc formation caused by $Fe(OH)_3$ precipitation at pH circa 6.8. The effluent however was turbid, with relatively high iron content, probably arising from collidal Fes
II. The blending of untreated AMD waters with H_2S recycle probably causes partial oxidation of H_2S to elemental sulphur, with Fe^{3+} acting as electron acceptor. The S^0 increases turbidity. More important however, reduction of Fe^{3+} to Fe^{2+} reduces the coagulation – flocullation efficacy of the Fe^{3+} in the untreated water
III. Raising the pH of the sulphide/amd blend to pH greater than 8 resulted in excellent iron removal, with a clear supernatant. This probably results from the coagulating properties of green rust, which coagulates iron sulphide colloids
IV. 90% of Mn and Zi were removed from the AMD water at the operational pH and the resultant colloids were probably flocculated by the green rust.